

AD 665828

NATURAL FREQUENCIES AND MODE SHAPES OF THE TRUNCATED CONICAL SHELL WITH FREE EDGES

PREPARED BY

FREDERICK A. KRAUSE
CAPTAIN, USAF

JANUARY 1968



HEADQUARTERS

SPACE AND MISSILE SYSTEMS ORGANIZATION

AIR FORCE SYSTEMS COMMAND

UNITED STATES AIR FORCE

THIS DOCUMENT HAS BEEN APPROVED FOR PUBLIC
RELEASE AND SALE; ITS DISTRIBUTION IS UNLIMITED

Air Force Report No.
SAMSO-TR-68-37

NATURAL FREQUENCIES AND MODE SHAPES
OF THE TRUNCATED CONICAL SHELL
WITH FREE EDGES

Prepared by
Frederick A. Krause
Captain, USAF

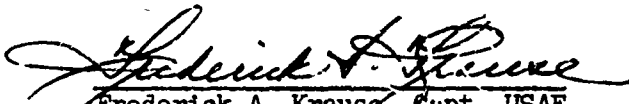
January 1968

Space and Missile Systems Organization
Air Force Systems Command
Los Angeles Air Force Station
Los Angeles, California

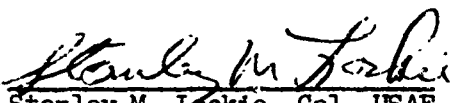
FOREWORD

This report presents a study accomplished by the author in partial fulfillment of the requirements for the degree of Doctor of Philosophy at the University of Arizona. The material contained in this report represents an updating and expansion of Air Force Report No. SSD-TR-66-201 of the same title and author published in October 1966.

Publication of this report does not constitute Air Force approval of the report's findings or conclusions. It is published only for the exchange and stimulation of ideas.


Frederick A. Krause, Capt, USAF
SAMSO(SMTAX)

Approved


Stanley M. Lockie, Col, USAF
Chief, Advanced Development Division (SMTA)
Directorate of Technology (SMT)

NATURAL FREQUENCIES AND MODE SHAPES
OF THE TRUNCATED CONICAL SHELL
WITH FREE EDGES

by
Frederick Arthur Krause

A Dissertation Submitted to the Faculty of the
DEPARTMENT OF AEROSPACE AND MECHANICAL ENGINEERING
In Partial Fulfillment of the Requirements
For the Degree of
DOCTOR OF PHILOSOPHY
In the Graduate College
THE UNIVERSITY OF ARIZONA

1968

STATEMENT BY AUTHOR

This dissertation has been submitted in partial fulfillment of requirements for an advanced degree at The University of Arizona and is deposited in the University Library to be made available to borrowers under rules of the Library.

Brief quotations from this dissertation are allowable without special permission, provided that accurate acknowledgment of source is made. Requests for permission for extended quotation from or reproduction of this manuscript in whole or in part may be granted by the head of the major department or the Dean of the Graduate College when in his judgment the proposed use of the material is in the interests of scholarship. In all other instances, however, permission must be obtained from the author.

SIGNED

Frederick Arthur Jones

ACKNOWLEDGMENTS

The author wishes to thank Dr. R. A. Anderson who supervised this investigation. This dissertation would not have been completed without his advice and encouragement.

The author also wishes to express his gratitude to the Western Processing Center at the University of California, Los Angeles, for use of the IBM 7094 computer utilized in this study.

TABLE OF CONTENTS

	Page
LIST OF ILLUSTRATIONS	v
LIST OF TABLES	vi
ABSTRACT	vii
CHAPTER	
I INTRODUCTION	1
II EQUATIONS OF MOTION AND BOUNDARY CONDITIONS	5
III SOLUTION OF THE EQUATIONS	16
Form of Solutions	16
Application of the Galerkin Procedure	21
IV COMPUTATIONAL PROCEDURE	34
Choice of Functions	34
Arranging the Equations for Computer Solution	36
Accuracy of Computational Procedure	39
V COMPARISON OF ANALYTICAL RESULTS WITH THE EXPERIMENTAL DATA OF HU, GORMLEY, AND LINDHOLM	43
VI COMPARISON OF ANALYTICAL RESULTS WITH THE EXPERIMENTAL DATA OF WATKINS AND CLARY	54
VII CONCLUSIONS	64
APPENDICES	67
APPENDIX A COMPLETE FLUGGE EQUATIONS	67
APPENDIX B FORTRAN COMPUTER PROGRAM	70
APPENDIX C COUPLING OF MODES	83
SYMBOLS	87
REFERENCES	89

LIST OF ILLUSTRATIONS

Figure		Page
2.1	Coordinates	6
2.2	Element Forces	9
5.1	First Mode Radial Displacement Shapes, Case 3	47
5.2	Second Mode Radial Displacement Shapes, Case 3	48
5.3	Comparison of Shapes	50
5.4	Effect of Varying Completeness Parameter . . .	52
6.1	Frequency Parameter, Case 5	56
6.2	Frequency Parameter, Case 6	57
6.3	Frequency Parameter, Case 7	58
6.4	Frequency Parameter, Case 8	59
6.5	Normalized Radial Displacements, Case 8 . . .	62

LIST OF TABLES

Table		Page
I	Normalized Frequencies for Three and Four Term Polynomials	41
II	Cone Geometry, Cases of Hu, Gormley, and Lindholm	43
III	Frequency Parameters, Case 1	45
IV	Frequency Parameters, Case 2	45
V	Frequency Parameters, Case 3	46
VI	Frequency Parameters, Case 4	46
VII	Cone Geometry, Cases of Watkins and Clary . .	55

ABSTRACT

Results from experimental studies concerning the natural frequencies and mode shapes of the thin truncated conical shell with free edge conditions have not been consistent. Mode shapes from one study were found to have an equal number of nodes at the two free cone edges when vibrating in a given mode while in contrast a second study revealed an unequal number of nodes at the edges. The theoretical results presented in this investigation are obtained through the use of a modified Galerkin procedure and are in agreement with the equal node experimental data. At the same time, the theoretical results have been used as a basis for explaining the opposing experimental data.

CHAPTER I

INTRODUCTION

The subject of conical shell vibrations has received very limited attention in the literature until recently. Although the conical shell has probably the simplest geometry, with the exception of cylindrical and spherical shells, the mathematical analysis of a conical shell is more difficult due to the fact that the governing differential equations of motion have variable coefficients. Consequently, most analyses of the vibrations of conical shells are accomplished through the use of approximate methods and numerical procedures for which large digital computers are a tremendous aid.

A comprehensive summary of significant previous works is given by Hu (4)¹. The majority of analyses concerning the natural frequencies and mode shapes of truncated conical shells concern those cases where the shell is fixed at one edge and free at the other, or simply supported at both edges. A recent work by Platus (9) is an example of a modern treatment of the fixed-free case,

1. Numbers in parentheses refer to the list of references.

wherein a digital computer and matrix methods are utilized. However, the case where both edges of the truncated conical shell are free of external support has not received similar analytical attention. Perhaps the reason is that it is difficult to choose functions which satisfy force type boundary conditions of the free-free case.

Recent experimental studies for the case of free-free edge conditions have been made by Watkins and Clary (12) and Hu, Gormley and Lindholm (6). Watkins and Clary observed that at certain natural frequencies a greater number of circumferential nodes occurred at the major end than at the minor end of the shell. This observation has generated some discussion in the literature [see Hu (5)] concerning the validity of the results. In the experimental work of Hu, et al., the phenomenon of different numbers of circumferential waves at the cone edges was not observed.

At the time this study was begun, the results of Hu, et al. were not available. The objective of the investigation at that time was to investigate the possibility that pure modes existed having nodal lines which are not generators of the cone, i.e., correlate theoretical analysis with the experimental data of Watkins and Clary. However, the analysis, wherein the assumed displacement shapes permitted an unequal number of circumferential waves

at the two edges of the cone, revealed an uncoupling such that a pure mode having an unequal number of nodes at the cone edges is not possible.

With the advent of the experimental results of Hu, Gormley and Lindholm, a controversy arose since their work did not reveal different numbers of circumferential waves at the two cone edges in a given vibration mode. The objective of the study at hand was therefore altered toward the direction of attempting to explain the apparent controversy between the two experimental studies.

In this investigation an approximate solution for the free-free case is obtained utilizing a modified Galerkin procedure wherein functions assumed in the solution need satisfy only the displacement boundary conditions, a feature of considerable advantage for the free-free case. The method accounts for errors in the forces and moments which result when the assumed functions do not satisfy the force type boundary conditions.

The theoretical analyses proceeded with the computer programming of the computational procedure described in Chapter IV. Results from the program for the experimental case of Hu, et al. showed good agreement with the experimental data both in frequencies and mode shapes. This correlation of results is presented in Chapter V.

A plausible explanation of the experimental results of Watkins and Clary, based upon specific computer results, is presented in Chapter VI.

CHAPTER II

EQUATIONS OF MOTION AND BOUNDARY CONDITIONS

The differential equations of motion utilized in this investigation are those developed by Seide (10) from energy principles. They are identical to those used by Chao-t sien (2). Equivalent equations, based upon elemental equilibrium considerations, can be obtained using Flugge's (3) simplified version of the elastic law as applied to a thin conical shell of constant thickness. The equations apply to homogeneous isotropic conical shells of constant wall thickness and are based upon linear, small displacement shell theory and the assumptions of a large mean diameter to shell thickness ratio and negligible deformations due to transverse shear. For "thin" shell theory it is assumed here that $h / (s \sin \alpha) \ll 1$, where h , s and α are as defined in Figure 2.1. More complete Flugge equations are presented in Appendix A. Basically, the additional terms found in the more general equations represent higher order terms for the very thin truncated shells analyzed in this study.

Development of the equations based upon energy principles will be presented here. Expressions for the

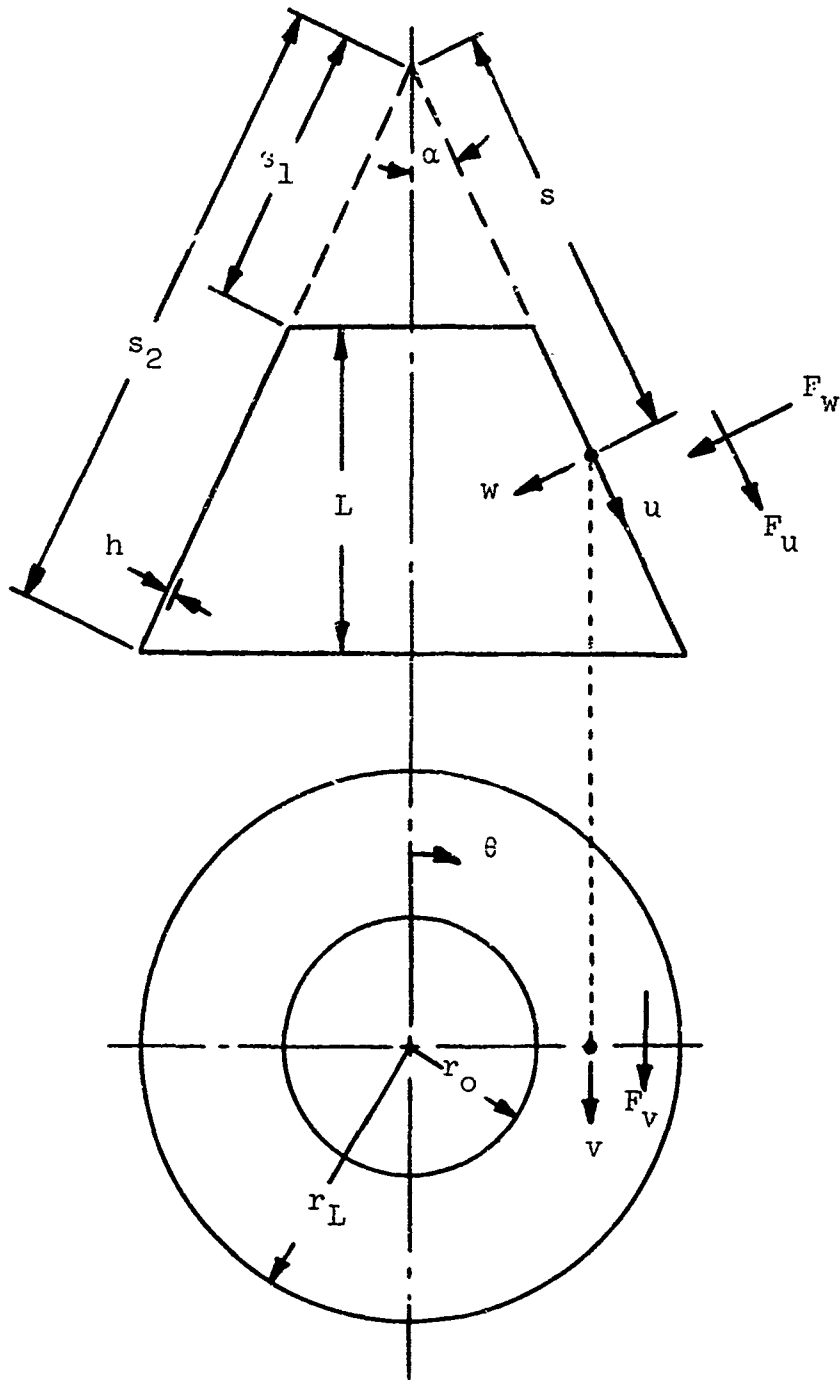


Figure 2.1 Coordinates

middle-surface strains and curvatures of a deformed conical shell as derived by Love (7) are given by

$$\epsilon_s = \frac{\partial u}{\partial s} \quad (2.1)$$

$$\epsilon_\theta = \frac{u - w \cot \alpha}{s} + \frac{1}{s \sin \alpha} \frac{\partial v}{\partial \theta} \quad (2.2)$$

$$\gamma_{s\theta} = \frac{\partial v}{\partial s} - \frac{v}{s} + \frac{1}{s \sin \alpha} \frac{\partial u}{\partial \theta} \quad (2.3)$$

$$\chi_s = \frac{\partial^2 w}{\partial s^2} \quad (2.4)$$

$$\chi_\theta = \frac{1}{s} \frac{\partial w}{\partial s} + \frac{1}{s^2 \sin^2 \alpha} \frac{\partial^2 w}{\partial \theta^2} + \frac{\cos \alpha}{s^2 \sin^2 \alpha} \frac{\partial v}{\partial \theta} \quad (2.5)$$

$$\chi_{s\theta} = \frac{1}{\sin \alpha} \frac{\partial}{\partial s} \left[\frac{1}{s} \left(\frac{\partial w}{\partial \theta} + v \cos \alpha \right) \right] \quad (2.6)$$

where u , v , and w are the displacements in the longitudinal, circumferential, and radial directions, respectively (see Figure 2.1). Following Seide, the strains are retained in the form of Eqs. (2.1) to (2.3), but the curvatures are modified by deleting the terms involving the circumferential displacement since experience has shown that these terms are negligible for very thin shells, especially as α approaches 90° where they become identically zero. Expressions for curvatures are thus given by

$$\chi_s = \frac{\partial^2 w}{\partial s^2} \quad (2.7)$$

$$\chi_{\theta} = \frac{1}{s} \frac{\partial w}{\partial s} + \frac{1}{s^2 \sin^2 \alpha} \frac{\partial^2 w}{\partial \theta^2} \quad (2.8)$$

$$\chi_{s\theta} = \frac{1}{\sin \alpha} \frac{\partial}{\partial s} \left(\frac{1}{s} \frac{\partial w}{\partial \theta} \right) \quad (2.9)$$

Figure 2.2 shows the force and moment stress resultants acting on a differential shell element. Stress resultants, N_s , $N_{s\theta}$, and Q_s are forces per unit of circumferential length; N_{θ} , $N_{\theta s}$, and Q_{θ} are forces per unit of longitudinal length; M_s and $M_{s\theta}$ are moments per unit of circumferential length, and M_{θ} and $M_{\theta s}$ are moments per unit of longitudinal length. The equations relating the stress resultants to strains and curvatures are as given by Seide (10):

$$N_s = \frac{Eh}{1-\nu^2} (\epsilon_s + \nu\epsilon_{\theta}) \quad (2.10)$$

$$N_{\theta} = \frac{Eh}{1-\nu^2} (\epsilon_{\theta} + \nu\epsilon_s) \quad (2.11)$$

$$N_{s\theta} = N_{\theta s} = \frac{Eh}{2(1+\nu)} \gamma_{s\theta} \quad (2.12)$$

$$M_s = -\frac{Dh^2}{12} (\chi_s + \nu\chi_{\theta}) \quad (2.13)$$

$$M_{\theta} = -\frac{Dh^2}{12} (\chi_{\theta} + \nu\chi_s) \quad (2.14)$$

$$M_{s\theta} = -M_{\theta s} = \frac{Dh^2}{12} (1-\nu) \chi_{s\theta} \quad (2.15)$$

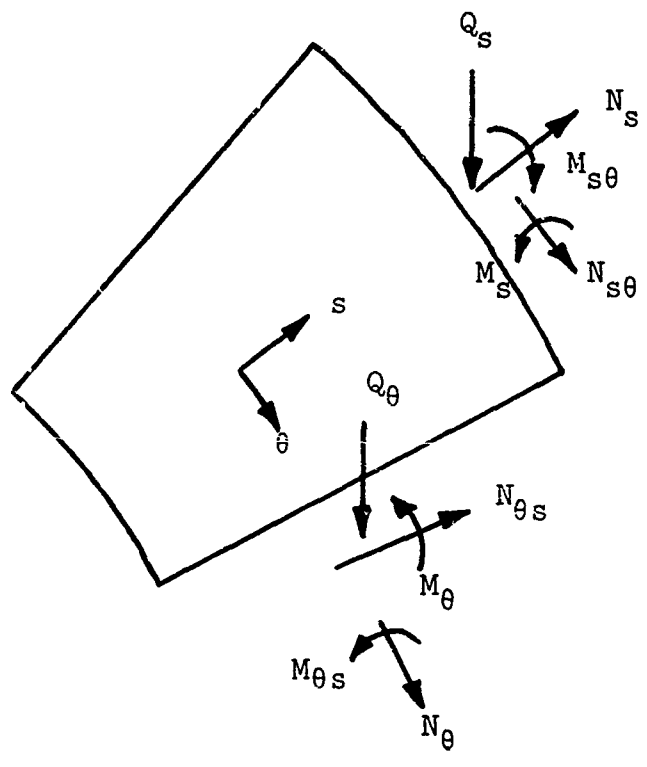


Figure 2.2 Element Forces

where E is Young's modulus, ν is Poisson's ratio, h is the shell thickness, and D is defined as

$$D = \frac{Eh}{(1-\nu^2)} \quad (2.16)$$

Equations of equilibrium and boundary conditions can be derived from energy principles. The total energy of a conical shell, i.e., the strain energy minus the work due to external forces, can be expressed for the complete circular shell as

$$\begin{aligned}
 U = & \int_0^{2\pi} \int_{s_1}^{s_2} \left[\frac{1}{2} (N_s \epsilon_s + N_\theta \epsilon_\theta + N_{s\theta} \gamma_{s\theta} - M_s \chi_s \right. \\
 & \left. - M_\theta \chi_\theta + 2M_{s\theta} \chi_{s\theta}) - (F_u u + F_v v + F_w w) s \sin \alpha \, ds d\theta \right. \\
 & \left. - \int_0^{2\pi} [s(\bar{N}_s u + \bar{N}_{s\theta} v - \bar{M}_s \frac{\partial w}{\partial s} + \bar{M}_{s\theta} \frac{1}{s \sin \alpha} \frac{\partial w}{\partial \theta} \right. \\
 & \left. + \bar{Q}_s w)] \Big|_{s_1}^{s_2} \sin \alpha \, d\theta \right] \quad (2.17)
 \end{aligned}$$

where F_u , F_v and F_w are external forces per unit of surface area and the barred stress resultants are forces or moments per unit length on the cone boundaries. Terms to be integrated along a longitudinal edge from s_1 to s_2 do not

appear since the development here is limited to a complete shell $\theta = 0$ to 2π . The terms, F_u , F_v and F_w , will later be replaced by inertia forces using D'Alembert's principle.

The energy expression in terms of the displacements, u , v , and w , is obtained by substituting the equations for stress resultants in terms of strains and curvatures, Eqs. (2.10) to (2.15), and strains and curvatures in terms of displacements, Eqs. (2.1) to (2.3) and (2.7) to (2.9), into the energy expression, Eq. (2.17). When the first variation of the resulting expression is taken and variations of the derivatives of displacements are eliminated through the use of integration by parts, Eq. (2.18) is obtained (written in terms of stress resultants).

$$\begin{aligned}
 \delta U = & - \int_0^{2\pi} \int_{s_1}^{s_2} \left\{ \left[\frac{\partial}{\partial s} (sN_s) - N_\theta + \frac{1}{\sin \alpha} \frac{\partial N_{s\theta}}{\partial \theta} + sF_u \right] \delta u \right. \\
 & + \left[\frac{1}{\sin \alpha} \frac{\partial N_\theta}{\partial \theta} + \frac{1}{s} \frac{\partial}{\partial s} (s^2 N_{s\theta}) + sF_v \right] \delta v \\
 & - \left[s \frac{Dh^2}{12} \nabla^4 w - N_\theta \cot \alpha - sF_w \right] \delta w \Big\} \sin \alpha \, ds d\theta \\
 & + \int_0^{2\pi} \left\{ s[(N_s - \bar{N}_s) \delta u + (N_{s\theta} - \bar{N}_{s\theta}) \delta v \right. \\
 & - (M_s - \bar{M}_s) \delta \left(\frac{\partial w}{\partial s} \right)] + \left[\frac{\partial}{\partial s} (sM_s) - M_\theta \right. \\
 & \left. - \frac{2}{\sin \alpha} \frac{\partial M_{s\theta}}{\partial \theta} - s\bar{Q}_s + \frac{1}{\sin \alpha} \frac{\partial \bar{M}_{s\theta}}{\partial \theta} \right] \delta w \Big\} \Big|_{s_1}^{s_2} \sin \alpha \, d\theta \quad (2.18)
 \end{aligned}$$

Again, terms to be integrated along a longitudinal shell edge do not appear because of the circumferential completeness of the shell. Here $\nabla^4 w$ is the usual cylindrical form

$$\nabla^4 w = \left(\frac{\partial^2}{\partial s^2} + \frac{1}{s} \frac{\partial}{\partial s} + \frac{1}{s^2 \sin^2 \alpha} \frac{\partial^2}{\partial \theta^2} \right) \left(\frac{\partial^2 w}{\partial s^2} + \frac{1}{s} \frac{\partial w}{\partial s} + \frac{1}{s^2 \sin^2 \alpha} \frac{\partial^2 w}{\partial \theta^2} \right) \quad (2.19)$$

The first variation of the energy δU must vanish for a minimum. Since δu , δv and δw are independent, each of the factors under the double integral must, therefore, vanish. In addition, the factors of each of the variations in the line integral must vanish independently. This procedure yields the set of equilibrium equations

$$(sN_s)' - N_\theta + \frac{N_s \dot{\theta}}{\sin \alpha} + sF_u = 0 \quad (2.20)$$

$$\frac{SN_\theta}{\sin \alpha} + (s^2 N_{s\theta})' + s^2 F_v = 0 \quad (2.21)$$

$$-s \frac{Dh^2}{12} \nabla^4 w + N_\theta \cot \alpha + sF_w = 0 \quad (2.22)$$

and the boundary conditions along $s = s_1$ and $s = s_2$

$$N_s = \bar{N}_s \equiv \bar{N} \quad \text{or} \quad u = 0 \quad (2.23)$$

$$N_{s\theta} = \bar{N}_{s\theta} \equiv \bar{T} \quad \text{or} \quad v = 0 \quad (2.24)$$

$$\begin{aligned} \frac{1}{s} [(sM_s)' - M_\theta - 2M_{s\theta} \csc \alpha] \\ = \frac{1}{s} [s\bar{Q}_s - \csc \alpha \bar{M}_{s\theta}] \equiv \bar{S} \quad \text{or} \quad w = 0 \end{aligned} \quad (2.25)$$

$$M_s = \bar{M}_s \equiv \bar{M} \quad \text{or} \quad w' = 0 \quad (2.26)$$

where \bar{N} , \bar{T} , \bar{S} , and \bar{M} are the generalized boundary forces associated with u , v , w , and w' , respectively. Generalized boundary forces here are both forces and moments per unit length along the shell edge. The indicated derivatives are defined by the notation

$$\frac{\partial}{\partial s} \equiv ()' \quad (2.27)$$

$$\frac{\partial}{\partial \theta} \equiv ()^\cdot \quad (2.28)$$

For the free-free case of no displacement constraints and no external edge forces, the boundary conditions become simply

$$N_s = 0 \quad \text{at} \quad s = s_1 \quad \text{and} \quad s_2 \quad (2.29)$$

$$N_{s\theta} = 0 \quad \text{at} \quad s = s_1 \quad \text{and} \quad s_2 \quad (2.30)$$

$$\frac{1}{s} [(sM_s)' - M_\theta - 2M_{s\theta} \csc \alpha] = 0 \text{ at } s = s_1 \text{ and } s_2 \quad (2.31)$$

$$M_s = 0 \text{ at } s = s_1 \text{ and } s_2 \quad (2.32)$$

For free vibrations the external forces per unit area, F_u , F_v , and F_w , are replaced by inertia forces using D'Alembert's principle. Rewriting the equations of equilibrium in terms of displacements such that they physically represent force per unit area in the longitudinal, circumferential, and radial directions, respectively, Eqs. (2.20) to (2.22) become

$$\begin{aligned} D \left[\frac{(1+\nu)}{2} \frac{v'}{s} \csc \alpha - \frac{(3-\nu)}{2} \frac{v'}{s^2} \csc \alpha + u'' \right. \\ \left. + \frac{(1-\nu)}{2} \frac{u''}{s^2} \csc^2 \alpha + \frac{u'}{s} - \frac{u}{s^2} - \frac{vw'}{s} \cot \alpha \right. \\ \left. + \frac{w}{s^2} \cot \alpha \right] - \rho h \frac{\partial^2 u}{\partial t^2} = 0 \end{aligned} \quad (2.33)$$

$$\begin{aligned} D \left[\frac{(1-\nu)}{2} v'' + \frac{v''}{s^2} \csc^2 \alpha + \frac{(1-\nu)}{2} \frac{v'}{s} - \frac{(1-\nu)}{2} \frac{v}{s^2} \right. \\ \left. + \frac{(1+\nu)}{2} \frac{u'}{s} \csc \alpha + \frac{(3-\nu)}{2} \frac{u'}{s^2} \csc \alpha - \frac{w'}{s^2} \cot \alpha \csc \alpha \right] \\ - \rho h \frac{\partial^2 v}{\partial t^2} = 0 \end{aligned} \quad (2.34)$$

$$\begin{aligned}
& D \left[\frac{v \cdot}{s^2} \csc \alpha + \frac{v}{s} u' + \frac{u}{s^2} - \frac{w}{s^2} \cot \alpha \right] \cot \alpha \\
& - \frac{Dh^2}{12} \left[w''' + 2 \frac{w' \cdot}{s^2} \csc^2 \alpha + \frac{w''}{s^4} \csc^4 \alpha \right. \\
& + \frac{2w'''}{s} - \frac{2w' \cdot}{s^3} \csc^2 \alpha - \frac{w''}{s^2} + \frac{4w''}{s^4} \csc^2 \alpha \\
& \left. + \frac{w'}{s^3} \right] - \rho h \frac{\partial^2 w}{\partial t^2} = 0 \tag{2.35}
\end{aligned}$$

where the constant ρ is the mass density. The boundary conditions, Eqs. (2.29) to (2.32), written in terms of displacements and units of generalized force per unit length, become

$$D \left[u' + v \left(\frac{u-w \cot \alpha}{s} + \frac{v \cdot}{s} \csc \alpha \right) \right] = 0 \tag{2.36}$$

$$D \left(\frac{1-v}{2} \right) \left[v' - \frac{v}{s} + \frac{u \cdot}{s} \csc \alpha \right] = 0 \tag{2.37}$$

$$\begin{aligned}
& - \frac{Dh^2}{12} \left[w''' + \frac{(2-v)}{s^2} w' \cdot \csc^2 \alpha - \frac{(3-v)}{s^3} w'' \csc^2 \alpha \right. \\
& \left. + \frac{w''}{s} - \frac{w'}{s^2} \right] = 0 \tag{2.38}
\end{aligned}$$

$$- \frac{Dh^2}{12} \left[w'' + v \left(\frac{w''}{s^2} \csc^2 \alpha + \frac{w'}{s} \right) \right] = 0 \tag{2.39}$$

CHAPTER III

SOLUTION OF THE EQUATIONS

Form of Solutions

As described briefly in Chapter I, the emphasis during the early phase of this study was to investigate the possibility (theoretically) that pure vibration modes of the form found by Watkins and Clary in their experimental work are possible. In order to permit solutions wherein a different number of nodes can occur at the two cone edges, consider complete Fourier series solutions of the form

$$u = \left[\sum_{n=0}^{\infty} U_n^{(1)}(s) \cos n\theta + \sum_{n=1}^{\infty} U_n^{(2)}(s) \sin n\theta \right] \sin \omega t \quad (3.1)$$

$$v = \left[\sum_{n=1}^{\infty} V_n^{(1)}(s) \sin n\theta + \sum_{n=0}^{\infty} V_n^{(2)}(s) \cos n\theta \right] \sin \omega t \quad (3.2)$$

$$w = \left[\sum_{n=0}^{\infty} W_n^{(1)}(s) \cos n\theta + \sum_{n=1}^{\infty} W_n^{(2)}(s) \sin n\theta \right] \sin \omega t \quad (3.3)$$

Regarding the functions, $U_n^{(1)}(s)$, $V_n^{(1)}(s)$, etc., to be arbitrary, this general form of solution has the property of completeness and can represent any possible mode exactly. Consider now the substitution of the solutions, Eqs. (3.1) to (3.3), into the first of the three applicable differential equations, Eq. (2.33). The result is given by Eq. (3.4).

$$\begin{aligned}
& D\left\{ \frac{(1+\nu)}{2} \frac{\csc\alpha}{s} \left[\sum_{n=1}^{\infty} n V_n^{(1)'} \cos n\theta + \sum_{n=0}^{\infty} n V_n^{(2)'} \sin n\theta \right] \right. \\
& - \frac{(3-\nu)}{2} \frac{\csc\alpha}{s^2} \left[\sum_{n=1}^{\infty} n V_n^{(1)} \cos n\theta + \sum_{n=0}^{\infty} n V_n^{(2)} \sin n\theta \right] \\
& + \left[\sum_{n=0}^{\infty} U_n^{(1)''} \cos n\theta + \sum_{n=1}^{\infty} U_n^{(2)''} \sin n\theta \right] \\
& - \frac{(1-\nu)}{2} \frac{\csc^2\alpha}{s^2} \left[\sum_{n=0}^{\infty} n^2 U_n^{(1)} \cos n\theta + \sum_{n=1}^{\infty} n^2 U_n^{(2)} \sin n\theta \right] \\
& + \frac{1}{s} \left[\sum_{n=0}^{\infty} U_n^{(1)} \cos n\theta + \sum_{n=1}^{\infty} U_n^{(2)} \sin n\theta \right] \\
& - \frac{1}{s^2} \left[\sum_{n=0}^{\infty} U_n^{(1)} \cos n\theta + \sum_{n=1}^{\infty} U_n^{(2)} \sin n\theta \right] \\
& - \frac{\nu \cot\alpha}{s} \left[\sum_{n=0}^{\infty} W_n^{(1)'} \cos n\theta + \sum_{n=1}^{\infty} W_n^{(2)'} \sin n\theta \right] \\
& + \frac{\cot\alpha}{s^2} \left[\sum_{n=0}^{\infty} W_n^{(1)} \cos n\theta + \sum_{n=1}^{\infty} W_n^{(2)} \sin n\theta \right] \} \\
& + \rho h w^2 \left[\sum_{n=0}^{\infty} U_n^{(1)} \cos n\theta + \sum_{n=1}^{\infty} U_n^{(2)} \sin n\theta \right] = 0 \quad (3.4)
\end{aligned}$$

Equation (3.4), plus two other similar equations which are obtained when the displacements, Eqs. (3.1) to (3.3), are substituted into the remaining equations of motion, Eqs. (2.34) and (2.35), are to be solved for the eigenfunctions $U_n^{(1)}(s)$, $V_n^{(1)}(s)$, etc. and the corresponding eigenvalues w^2 . Following the usual procedure,

these three equations are multiplied by either $\cos m\theta$ or $\sin m\theta$ and integrated from $\theta = 0$ to $\theta = 2\pi$. Consider, for example, the multiplication of Eq. (3.4) by $\cos m\theta$ and the subsequent integration from $\theta = 0$ to $\theta = 2\pi$. Due to orthogonality, the terms involving the functions with a superscript (2) are completely eliminated, the only remaining terms being those for which $n = m$ and involving the superscript (1). When both integrations are performed independently on each of the three equations, the result is six equations, three of which involve the functions $U_m^{(1)}(s)$, $V_m^{(1)}(s)$, and $W_m^{(1)}(s)$ while the remaining three involve the functions $U_m^{(2)}(s)$, $V_m^{(2)}(s)$, and $W_m^{(2)}(s)$. Furthermore, the three equations involving the functions with superscript (1) are identical with the three equations involving the superscript (2). Thus there is no need to consider both sets of functions. The family of modes for which $n = m$ is completely given by

$$u = U_m(s) \cos m\theta \sin \omega t \quad (3.5)$$

$$v = V_m(s) \sin m\theta \sin \omega t \quad (3.6)$$

$$w = W_m(s) \cos m\theta \sin \omega t \quad (3.7)$$

where m is the number of full waves around the circum-

ference of the shell, also defined by one-half the number of nodal points encountered when going around the circumference.

For the purpose of obtaining an approximate solution through the use of the Galerkin procedure, a finite series approximation of the form

$$u = \sum_{i=1}^n q_i \alpha_i(s) \cos m\theta \sin \omega t \quad (3.8)$$

$$v = \sum_{i=1}^n q_i \beta_i(s) \sin m\theta \sin \omega t \quad (3.9)$$

$$w = \sum_{i=1}^n q_i \gamma_i(s) \cos m\theta \sin \omega t \quad (3.10)$$

was used for this investigation. Here m is allowed to take on a single value for a specific solution. The choice of the functions $\alpha_i(s)$, $\beta_i(s)$ and $\gamma_i(s)$ are discussed further in Chapter IV. Modal patterns resulting from using these displacements will, of course, consist of parallel circles and equispaced meridians -- patterns which because of the axial symmetry of the shell and the boundary conditions, and the circumferential periodicity of the vibration motion, are entirely logical. The experimental investigation of Hu, Gormley, and Lindholm (6), conducted at the Southwest Research Institute, confirms the foregoing

discussion. Further details of these results appear in Chapter V.

Application of the Galerkin Procedure

The Galerkin procedure used by Bolotin (1) and Matthews (8) differs from the usual Galerkin procedure in that the functions utilized for the assumed solution must satisfy only the displacement or "natural" boundary conditions. This is an important feature since in the case of the free-free conical shell it is inconvenient to choose functions which satisfy the boundary conditions, Eqs. (2.36) to (2.39). In fact, it is difficult to find functions which do satisfy these boundary conditions. In this method the errors in the forces and moments at the boundaries are weighted along with the error functions from the differential equations. The total weighted error is then set equal to zero which is equivalent to setting the virtual work done by all the forces and moments moving through appropriate displacements equal to zero.

The modified Galerkin procedure requires additional equations to account for the boundary errors. The equations are obtained from the requirement that boundary forces and moments must balance the internal forces and moments on an infinitesimal end element. Utilizing the force type boundary conditions, Eqs. (2.36) to (2.39), in

equations of equilibrium written for an end element, the required equations for the end element at $s = s_1$ are given by Eqs. (3.11) to (3.14).

$$\left. \left\{ -\bar{N} + D \left[u' + \frac{\nu}{s} (u-w \cot \alpha) + \frac{\nu v \dot{v}}{s} \csc \alpha \right] \right\} \right|_{s=s_1} = 0 \quad (3.11)$$

$$\left. \left\{ -\bar{T} + \frac{D(1-\nu)}{2} \left[v' - \frac{v}{s} + \frac{u \dot{v}}{s} \csc \alpha \right] \right\} \right|_{s=s_1} = 0 \quad (3.12)$$

$$\left. \left\{ -\bar{S} - \frac{Dh^2}{12} \left[w''' + \frac{(2-\nu)}{s^2} w' \csc^2 \alpha - \frac{(3-\nu)}{s^3} w \csc^2 \alpha + \frac{w''}{s} - \frac{w'}{s^2} \right] \right\} \right|_{s=s_1} = 0 \quad (3.13)$$

$$\left. \left\{ \bar{M} + \frac{Dh^2}{12} \left[w'' + \nu \left(\frac{w \dot{v}}{s^2} \csc^2 \alpha + \frac{w'}{s} \right) \right] \right\} \right|_{s=s_1} = 0 \quad (3.14)$$

where \bar{N} , \bar{T} , \bar{S} , and \bar{M} are the generalized boundary forces per unit length as previously defined. Similarly, the set of equations for the other edge of the shell where $s = s_2$ is given by Eqs. (3.15) to (3.18). In Eqs. (3.11) to (3.14) above as well as in Eqs. (3.15) to (3.18) below, positive forces are generally taken to be in the direction

of positive displacements (see Figures 2.1 and 2.2). Care must be exercised in the determination of the signs of the forces at the shell boundaries. The signs which appear in these equations must be carried through the steps of the modified Galerkin procedure which follow.

$$\left\{ \bar{N} - D \left[u' + \frac{\nu}{s} (u - w \cot \alpha) + \frac{\nu v'}{s} \csc \alpha \right] \right\} \Big|_{s=s_2} = 0 \quad (3.15)$$

$$\left\{ \bar{T} - \frac{D(1-\nu)}{2} \left[v' - \frac{\nu}{s} + \frac{u'}{s} \csc \alpha \right] \right\} \Big|_{s=s_2} = 0 \quad (3.16)$$

$$\left\{ \bar{S} + \frac{Dh^2}{12} \left[w''' + \frac{(2-\nu)}{s^2} w'' \csc^2 \alpha - \frac{(3-\nu)}{s^3} w' \csc^2 \alpha + \frac{w''}{s} - \frac{w'}{s^2} \right] \right\} \Big|_{s=s_2} = 0 \quad (3.17)$$

$$\left\{ -\bar{M} - \frac{Dh^2}{12} \left[w'' + \nu \left(\frac{w'}{s^2} \csc^2 \alpha + \frac{w'}{s} \right) \right] \right\} \Big|_{s=s_2} = 0 \quad (3.18)$$

An exact solution must satisfy the end element equations, Eqs. (3.11) to (3.18), as well as the general element differential equations, Eqs. (2.33) to (2.35). The approximate solution to be considered here will not satisfy

all of these equations. Therefore, errors in all of them are to be accounted for in the modified Galerkin procedure.

A set of error functions is generated by the substitution of the assumed displacements, Eqs. (3.8) to (3.10), into the general equilibrium equations, Eqs. (2.33) to (2.35) and the boundary equilibrium equations, Eqs. (3.11) to (3.18). These are given by Eqs. (3.19) to (3.29) which follow.

$$\begin{aligned}
 & \cos m\theta \sin \omega t \sum_i q_i \left\{ D \left[\frac{(1+\nu)}{2} \frac{\csc \alpha}{s} m \beta_i' \right. \right. \\
 & - \frac{(3-\nu)}{2} \frac{\csc \alpha}{s^2} m \beta_i + \alpha_i'' - \frac{(1-\nu)}{2} \frac{\csc^2 \alpha}{s^2} m^2 \alpha_i + \frac{1}{s} \alpha_i' \\
 & \left. \left. - \frac{1}{s^2} \alpha_i - \frac{\nu \cot \alpha}{s} \gamma_i' + \frac{\cot \alpha}{s^2} \gamma_i \right] + \rho h \omega^2 \alpha_i \right\} \\
 & = \epsilon_\alpha(s, \theta) \qquad (3.19)
 \end{aligned}$$

$$\begin{aligned}
 & \sin m\theta \sin \omega t \sum_i q_i \left\{ D \left[\frac{(1-\nu)}{2} \beta_i'' - \frac{\csc^2 \alpha}{s^2} m^2 \beta_i \right. \right. \\
 & + \frac{(1-\nu)}{2s} \beta_i' - \frac{(1-\nu)}{2s^2} \beta_i - \frac{(1+\nu)}{2} \frac{\csc \alpha}{s} m \alpha_i' \\
 & \left. \left. - \frac{(3-\nu)}{2} \frac{\csc \alpha}{s^2} m \alpha_i + \frac{\cot \alpha \csc \alpha}{s^2} m \gamma_i \right] \right. \\
 & \left. + \rho h \omega^2 \beta_i \right\} = \epsilon_\beta(s, \theta) \qquad (3.20)
 \end{aligned}$$

$$\begin{aligned}
& \cos m\theta \sin \omega t \sum_i q_i \left\{ D \left[\frac{\csc \alpha}{s^2} m\beta_i + \frac{v}{s} \alpha_i' \right. \right. \\
& + \left. \frac{1}{s^2} \alpha_i - \frac{\cot \alpha}{s^2} \gamma_i \right] \cot \alpha - \frac{Dh^2}{12} [\gamma_i'''' - \frac{2\csc^2 \alpha}{s^2} m^2 \gamma_i'' \\
& + \frac{\csc^4 \alpha}{s^4} m^4 \gamma_i + \frac{2}{s} \gamma_i'''' + \frac{2\csc^2 \alpha}{s^3} m^2 \gamma_i' - \frac{1}{s^2} \gamma_i'' \\
& \left. - \frac{4\csc^2 \alpha}{s^4} m^2 \gamma_i + \frac{1}{s^3} \gamma_i'] + \rho h \omega^2 \gamma_i \right\} = \epsilon_Y(s, \theta) \quad (3.21)
\end{aligned}$$

$$\begin{aligned}
& - \bar{N} + \cos m\theta \sin \omega t \sum_i q_i \left\{ D \left[\alpha_i' + \frac{v}{s} (\alpha_i - \gamma_i \cot \alpha \right. \right. \\
& \left. \left. + \csc \alpha m\beta_i) \right] \right\} \Bigg|_{s=s_1} = E_1(\theta) \quad (3.22)
\end{aligned}$$

$$\begin{aligned}
& \bar{N} - \cos m\theta \sin \omega t \sum_i q_i \left\{ D \left[\alpha_i' + \frac{v}{s} (\alpha_i - \gamma_i \cot \alpha \right. \right. \\
& \left. \left. + \csc \alpha m\beta_i) \right] \right\} \Bigg|_{s=s_2} = E_2(\theta) \quad (3.23)
\end{aligned}$$

$$\begin{aligned}
& - \bar{T} + \sin m\theta \sin \omega t \sum_i q_i \left\{ \frac{D(1-\nu)}{2} [\beta_i' - \frac{1}{s} \beta_i \right. \\
& \left. - \frac{\csc \alpha}{s} m \alpha_i] \right\} \Bigg|_{s=s_1} = E_3(\theta) \quad (3.24)
\end{aligned}$$

$$\begin{aligned}
& \bar{T} - \sin m\theta \sin \omega t \sum_i q_i \left\{ \frac{D(1-\nu)}{2} [\beta_i' - \frac{1}{s} \beta_i \right. \\
& \left. - \frac{\csc \alpha}{s} m \alpha_i] \right\} \Bigg|_{s=s_2} = E_4(\theta) \quad (3.25)
\end{aligned}$$

$$\begin{aligned}
& - \bar{S} - \cos m\theta \sin \omega t \sum_i q_i \left\{ \frac{Dh^2}{12} [\gamma_i''' - \frac{(2-\nu)}{s^2} \csc^2 \alpha m^2 \gamma_i' \right. \\
& \left. + \frac{(3-\nu)}{s^3} \csc^2 \alpha m^2 \gamma_i + \frac{\gamma_i''}{s} - \frac{1}{s^2} \gamma_i'] \right\} \Bigg|_{s=s_2} = E_5(\theta) \quad (3.26)
\end{aligned}$$

$$\begin{aligned}
& \bar{S} + \cos m\theta \sin \omega t \sum_i q_i \left\{ \frac{Dh^2}{12} [\gamma_i''' - \frac{(2-\nu)}{s^2} \csc^2 \alpha m^2 \gamma_i' \right. \\
& \left. + \frac{(3-\nu)}{s^3} \csc^2 \alpha m^2 \gamma_i + \frac{\gamma_i''}{s} - \frac{1}{s^2} \gamma_i'] \right\} \Bigg|_{s=s_2} = E_6(\theta) \quad (3.27)
\end{aligned}$$

$$\bar{M} + \cos m\theta \sin \omega t \sum_1 q_1 \left\{ \frac{Dh^2}{12} [\gamma_1'' + \nu \left(-\frac{\csc^2 \alpha}{s^2} m^2 \gamma_1 + \frac{1}{s} \gamma_1' \right) \right\} \Big|_{s=s_1} = E_7(\theta) \quad (3.28)$$

$$-\bar{M} - \cos m\theta \sin \omega t \sum_1 q_1 \left\{ \frac{Dh^2}{12} [\gamma_1'' + \nu \left(-\frac{\csc^2 \alpha}{s^2} m^2 \gamma_1 + \frac{1}{s} \gamma_1' \right) \right\} \Big|_{s=s_2} = E_8(\theta) \quad (3.29)$$

In the modified Galerkin procedure, the error functions representing the end errors, Eqs. (3.22) to (3.29), are weighted by displacements in a manner similar to the weighting of the error functions, Eqs. (3.19) to (3.21), resulting from the differential equations of motion. Error functions, $\epsilon_\alpha(s, \theta)$, $E_1(\theta)$, and $E_2(\theta)$, which represent errors in force in the longitudinal direction, will be multiplied by the displacement u per unit displacement of the j^{th} coordinate. Similarly, $\epsilon_\beta(s, \theta)$, $E_3(\theta)$, and $E_4(\theta)$, which represent errors in force in the circumferential direction, will be multiplied by the displacement v per unit displacement of the j^{th} coordinate;

and $\epsilon_\gamma(s, \theta)$, $E_5(\theta)$, and $E_6(\theta)$, which represent errors in force in the radial direction, will be multiplied by the displacement w per unit displacement of the j^{th} coordinate. Functions $E_7(\theta)$ and $E_8(\theta)$, which represent errors in moment, will be multiplied by the rate of change of radial displacement in the longitudinal direction $\partial w / \partial s$ per unit in the j^{th} coordinate. The sum of all these weighted errors, integrated over the entire conical shell, will be set equal to zero. Written in terms of the error functions defined previously, application of the foregoing procedure yields the j^{th} equation, Eq. (3.30).

$$\begin{aligned}
 & \int_0^{2\pi} \int_{s_1}^{s_2} [\epsilon_\alpha \alpha_j \cos m\theta + \epsilon_\beta \beta_j \sin m\theta + \epsilon_\gamma \gamma_j \cos m\theta] s \sin \alpha \, d\theta ds \\
 & + \int_0^{2\pi} [E_1 \alpha_j \cos m\theta \Big|_{s=s_1} + E_2 \alpha_j \cos m\theta \Big|_{s=s_2} \\
 & + E_3 \beta_j \sin m\theta \Big|_{s=s_1} + E_4 \beta_j \sin m\theta \Big|_{s=s_2} + E_5 \gamma_j \cos m\theta \Big|_{s=s_1} \\
 & + E_6 \gamma_j \cos m\theta \Big|_{s=s_2} + E_7 \gamma_j' \cos m\theta \Big|_{s=s_1} \\
 & + E_8 \gamma_j' \cos m\theta \Big|_{s=s_2}] s \sin \alpha \, d\theta = 0 \qquad (3.30)
 \end{aligned}$$

The foregoing procedure is equivalent to applying the principle of virtual work, i.e., requiring that the virtual work done by the forces and moments in a displacement in the j^{th} coordinate be equal to zero. Expanding Eq. (3.30) through the use of the error functions, Eqs. (3.19) to (3.29), integrating the result over θ and cancelling terms, the general i^{th} term in the j^{th} equation can be expressed as

$$\begin{aligned}
 & \int_{s_1}^{s_2} \left\{ \frac{(1+\nu)}{2} \frac{\csc \alpha}{s} m \beta_i' \alpha_j - \frac{(3-\nu)}{2} \frac{\csc \alpha}{s^2} m \beta_i \alpha_j + \alpha_i'' \alpha_j \right. \\
 & - \frac{(1-\nu)}{2} \frac{\csc^2 \alpha}{s^2} m^2 \alpha_i \alpha_j + \frac{1}{s} \alpha_i' \alpha_j - \frac{\nu \cot \alpha}{s} \gamma_i' \alpha_j - \frac{1}{s^2} \alpha_i \alpha_j \\
 & + \frac{\cot \alpha}{s^2} \gamma_i \alpha_j + \rho \frac{(1-\nu^2)}{E} \omega^2 \alpha_i \alpha_j + \frac{(1-\nu)}{2} \beta_i'' \beta_j \\
 & - \frac{\csc^2 \alpha}{s^2} m^2 \beta_i \beta_j + \frac{(1-\nu)}{2s} \beta_i' \beta_j - \frac{(1-\nu)}{2s^2} \beta_i \beta_j \\
 & - \frac{(1+\nu)}{2} \frac{\csc \alpha}{s} m \alpha_i' \beta_j - \frac{(3-\nu)}{2} \frac{\csc \alpha}{s^2} m \alpha_i \beta_j \\
 & + \frac{\cot \alpha \csc \alpha}{s^2} m \gamma_i \beta_j + \rho \frac{(1-\nu^2)}{E} \omega^2 \beta_i \beta_j + \left[\frac{\csc \alpha}{s^2} m \beta_i \gamma_j \right. \\
 & \left. + \frac{\nu}{s} \alpha_i' \gamma_j + \frac{1}{s^2} \alpha_i \gamma_j - \frac{\cot \alpha}{s^2} \gamma_i \gamma_j \right] \cot \alpha - k [\gamma_i'''' \gamma_j
 \end{aligned}$$

$$\begin{aligned}
& - \frac{2 \csc^2 \alpha}{s^2} m^2 \gamma_i''' \gamma_j + \frac{\csc^4 \alpha}{s^4} m^4 \gamma_i \gamma_j + \frac{2}{s} \gamma_i''' \gamma_j \\
& + \frac{2 \csc^2 \alpha}{s^3} m^2 \gamma_i' \gamma_j - \frac{1}{s^2} \gamma_i'' \gamma_j - \frac{4 \csc^2 \alpha}{s^4} m^2 \gamma_i \gamma_j \\
& + \frac{1}{s^3} \gamma_i' \gamma_j + \rho \frac{(1-v^2)}{E} \omega^2 \gamma_i \gamma_j \} s \sin \alpha \, ds \\
& + \left[\alpha_i' \alpha_j + \frac{v \alpha_i \alpha_j}{s} - \frac{v \cot \alpha}{s} \alpha_j + \frac{v \csc \alpha}{s} m \beta_i \alpha_j \right] s \sin \alpha \Big|_{s_1} \\
& - \left[\alpha_i' \alpha_j + \frac{v \alpha_i \alpha_j}{s} - \frac{v \cot \alpha}{s} \alpha_j + \frac{v \csc \alpha}{s} m \beta_i \alpha_j \right] s \sin \alpha \Big|_{s_2} \\
& + \frac{(1-v)}{2} \left[\beta_i' \beta_j - \frac{1}{s} \beta_i \beta_j - \frac{\csc \alpha}{s} m \alpha_i \beta_j \right] s \sin \alpha \Big|_{s_1} \\
& - \frac{(1-v)}{2} \left[\beta_i' \beta_j - \frac{1}{s} \beta_i \beta_j - \frac{\csc \alpha}{s} m \alpha_i \beta_j \right] s \sin \alpha \Big|_{s_2} \\
& + k \left[\gamma_i'' \gamma_j' - \frac{v \csc^2 \alpha}{s^2} m^2 \gamma_i \gamma_j' + \frac{v}{s} \gamma_i' \gamma_j' \right] s \sin \alpha \Big|_{s_1} \\
& - k \left[\gamma_i'' \gamma_j' - \frac{v \csc^2 \alpha}{s^2} m^2 \gamma_i \gamma_j' + \frac{v}{s} \gamma_i' \gamma_j' \right] s \sin \alpha \Big|_{s_2}
\end{aligned}$$

$$\begin{aligned}
& - k [\gamma_i''' \gamma_j - \frac{(2-\nu)}{s^2} \csc^2 \alpha m^2 \gamma_i' \gamma_j + \frac{(3-\nu)}{s^3} \csc^2 \alpha m^2 \gamma_i \gamma_j \\
& + \frac{\gamma_i'' \gamma_j}{s} - \frac{1}{s^2} \gamma_i' \gamma_j] s \sin \alpha \Big|_{s_1} + k [\gamma_i''' \gamma_j \\
& - \frac{(2-\nu)}{s^2} \csc^2 \alpha m^2 \gamma_i' \gamma_j + \frac{(3-\nu)}{s^3} \csc^2 \alpha m^2 \gamma_i \gamma_j + \frac{\gamma_i'' \gamma_j}{s} \\
& - \frac{1}{s^2} \gamma_i' \gamma_j] s \sin \alpha \Big|_{s_2} \tag{3.31}
\end{aligned}$$

where k is defined as

$$k = \frac{h^2}{12} \tag{3.32}$$

and the generalized external boundary forces at $s=s_1$ and $s=s_2$, i.e., \bar{N} , \bar{T} , \bar{S} , and \bar{M} , are taken to be zero.

Through the use of integration by parts, the general i_j^{th} term may be written in the symmetric form

$$\begin{aligned}
& \int_{s_1}^{s_2} \left\{ \left[\rho \frac{(1-\nu^2)}{E} \omega^2 s - \frac{1}{s} \left(1 + \frac{(1-\nu)}{2} m^2 \csc^2 \alpha \right) \right] \alpha_i \alpha_j \right. \\
& \left. - s \alpha_i' \alpha_j' + \left[\rho \frac{(1-\nu^2)}{E} \omega^2 s - \frac{1}{s} \left(\frac{(1-\nu)}{2} + m^2 \csc^2 \alpha \right) \right] \beta_i \beta_j \right.
\end{aligned}$$

$$\begin{aligned}
& - \frac{(1-\nu)}{2} s \beta_i' \beta_j' + \left[\rho \frac{(1-\nu^2)}{E} \omega^2 s - \frac{\cot^2 \alpha}{s} \right. \\
& - \frac{km^2 \csc^2 \alpha}{s^3} (m^2 \csc^2 \alpha - 4) \left. \right] \gamma_i \gamma_j - \frac{k}{s} (2m^2 \csc^2 \alpha + 1) \gamma_i' \gamma_j' \\
& - k s \gamma_i'' \gamma_j'' - \frac{(3-\nu)}{2} \frac{m \csc \alpha}{s} (\alpha_i \beta_j + \beta_i \alpha_j) \\
& + \frac{(1+\nu)}{2} m \csc \alpha (\alpha_i \beta_j' + \beta_i' \alpha_j) + \frac{\cot \alpha}{s} (\alpha_i \gamma_j + \gamma_i \alpha_j) \\
& + \nu \cot \alpha (\alpha_i' \gamma_j + \gamma_i' \alpha_j') + \frac{m \cot \alpha \csc \alpha}{s} (\gamma_i \beta_j + \beta_i \gamma_j) \} ds \\
& + \left\{ - \nu \alpha_i \alpha_j + \frac{(1-\nu)}{2} \beta_i \beta_j + \frac{km^2 (3-\nu) \csc^2 \alpha}{s^2} \gamma_i \gamma_j \right. \\
& + \frac{k m^2 \csc^2 \alpha}{s} (\gamma_i \gamma_j' + \gamma_i' \gamma_j) - k \nu \gamma_i' \gamma_j' \\
& \left. - \nu m \csc \alpha (\alpha_i \beta_j + \beta_i \alpha_j) \right\} \Big|_{s_1}^{s_2} \tag{3.33}
\end{aligned}$$

Equation (3.33), which is the basis for all calculations that follow, may also be derived using the Rayleigh-Ritz procedure beginning with an energy expression of the form

$$\begin{aligned}
 U = & \int_0^{2\pi} \int_{s_1}^{s_2} \frac{1}{2} [D (\epsilon_s^2 + \epsilon_\theta^2 + 2\nu\epsilon_s\epsilon_\theta + \frac{(1-\nu)}{2} \gamma_{s\theta}^2 \\
 & + kD (K_s^2 + K_\theta^2 + 2\nu K_s K_\theta + 2(1-\nu) K_{s\theta}^2 \\
 & - (F_u u + F_v v + F_w w)] s \sin \alpha \, ds d\theta \quad (3.34)
 \end{aligned}$$

and utilizing the strains, Eqs. (2.1) to (2.3), and the curvatures, Eqs. (2.7) to (2.9). Details of this derivation will not be presented here. The Galerkin and Rayleigh-Ritz procedures are equivalent when the differential equations of equilibrium used in the Galerkin method are obtained from a variation of the energy expression used in the Rayleigh-Ritz procedure. This was pointed out by Singer (11).

CHAPTER IV

COMPUTATIONAL PROCEDURE

Choice of Functions

For the case of a conical shell free of edge supports, the choice of displacement functions in the longitudinal direction, $\alpha_i(s)$, $\beta_i(s)$ and $\gamma_i(s)$, are somewhat arbitrary since the displacement boundary conditions are completely relaxed. Polynomials have been used by several investigators, i.e., Platus (9), for the case of fixed-end conditions on one cone edge. Because of the great number of integrations that must be performed to determine the matrix coefficients, it was decided to also utilize polynomials. There are, of course, other possibilities such as the functions which might be obtained from the free vibrations of a tapered beam without end supports. However, the necessary integrations would be unwieldy.

Third degree polynomials of the form of Eqs. (4.1) to (4.3) were assumed in the determination of the results presented in this study. Higher degree polynomials are better able to represent the more complex shapes of modes higher than the third. On the other hand, the

size of the matrix which must be inverted is increased by three rows and columns for each added degree, a factor which reduces computational accuracy. Primary interest was in the first two modes for each case of a fixed number of circumferential waves. Therefore a degree high enough to adequately represent the lower modes was determined to be the logical choice for this investigation. Further discussion on computational accuracy is given later in this chapter.

$$\alpha_i = \left(\frac{s}{s_2}\right)^{i-1} \quad i = 1 \text{ to } 4 \quad (4.1)$$

$$\beta_i = \left(\frac{s}{s_2}\right)^{i-5} \quad i = 5 \text{ to } 8 \quad (4.2)$$

$$\gamma_i = \left(\frac{s}{s_2}\right)^{i-9} \quad i = 9 \text{ to } 12 \quad (4.3)$$

Other functions, i.e., α_5 , α_6 , β_1 , β_2 , etc., were taken to be zero. This seemingly odd indexing was necessary in order to assemble the matrix elements.

Arranging the Equations for Computer Solution

The n homogeneous equations which result from the application of the modified Galerkin procedure to the problem of free vibrations of a thin truncated conical shell can be expressed in the matrix form

$$\rho \frac{(1-\nu^2)}{E} \omega^2 [M] \begin{Bmatrix} q_1 \\ \vdots \\ q_2 \end{Bmatrix} - [K] \begin{Bmatrix} q_1 \\ \vdots \\ q_2 \end{Bmatrix} = \begin{Bmatrix} 0 \\ \vdots \\ 0 \end{Bmatrix} \quad (4.4)$$

where the generalized mass matrix $[M]$, determined from the general i_j^{th} term, Eq. (3.33), is

$$M_{ij} = \int_{s_1}^{s_2} (\alpha_i \alpha_j + \beta_i \beta_j + \gamma_i \gamma_j) s ds \quad (4.5)$$

and the generalized stiffness matrix $[K]$, also determined from Eq. (3.33), is

$$\begin{aligned}
K_{ij} = & - \int_{s_1}^{s_2} \left\{ -\frac{1}{s} \left[1 + \frac{(1-\nu)}{2} m^2 \csc^2 \alpha \right] \alpha_i \alpha_j \right. \\
& - s \alpha_i' \alpha_j' - \frac{1}{s} \left[\frac{(1-\nu)}{2} + m^2 \csc^2 \alpha \right] \beta_i \beta_j \\
& - \frac{(1-\nu)}{2} s \beta_i' \beta_j' - \left[\frac{\cot^2 \alpha}{s} + \frac{km^2 \csc^2 \alpha}{s^3} (m^2 \csc^2 \alpha - 4) \right] \gamma_i \gamma_j \\
& - \frac{k}{s} (2m^2 \csc^2 \alpha + 1) \gamma_i' \gamma_j' - k s \gamma_i'' \gamma_j'' \\
& - \frac{(3-\nu)m \csc \alpha}{2s} (\alpha_i \beta_j + \beta_i \alpha_j) + \frac{(1+\nu)m \csc \alpha}{2} (\alpha_i \beta_j' + \beta_i' \alpha_j) \\
& + \frac{\cot \alpha}{s} (\alpha_i \gamma_j + \gamma_i \alpha_j) + \nu \cot \alpha (\alpha_i' \gamma_j + \gamma_i' \alpha_j') \\
& + \frac{m \cot \alpha \csc \alpha}{s} (\gamma_i \beta_j + \beta_i \gamma_j) \Big\} ds + \{-\nu \alpha_i \alpha_j \\
& + \frac{(1-\nu)}{2} \beta_i \beta_j + \frac{km^2(3-\nu) \csc^2 \alpha}{s^2} \gamma_i \gamma_j \\
& + \frac{k \nu m^2 \csc^2 \alpha}{s} (\gamma_i \gamma_j' + \gamma_i' \gamma_j) - k \nu \gamma_i' \gamma_j' \\
& - \nu m \csc \alpha (\alpha_i \beta_j + \beta_i \alpha_j) \Big\} \Big|_{s_1}^{s_2} \quad (4.6)
\end{aligned}$$

Having chosen the functions α_i , β_i and γ_i , the above mass and stiffness matrix elements can be evaluated for a shell having specified geometry and a fixed number of circumferential waves, m .

In order to solve this problem numerically on a digital computer, matrix Eq. (4.4) can be more favorably rewritten as

$$\frac{1}{\rho(1-\nu^2)\omega^2/E} \begin{Bmatrix} q_1 \\ \vdots \\ q_n \end{Bmatrix} = [K]^{-1} [M] \begin{Bmatrix} q_1 \\ \vdots \\ q_n \end{Bmatrix} \quad (4.7)$$

where $[K]^{-1}$ is the inverse of the matrix $[K]$. Equation (4.7) is solved through a process of matrix iteration which produces the n frequencies and corresponding mode shapes for the simplified constrained system. After the fundamental frequency and mode shape is found, a process of matrix sweeping is utilized to remove the first mode, thereby allowing the second iteration process to converge on the second mode. This technique is continued until as many frequencies and mode shapes as are desired have been determined, up to a maximum of n . Computations were accomplished on the IBM 7072 computer at The University of Arizona and the IBM 7094 computer at the Western Data Processing Center, University of California at Los Angeles. The program is similar to that used by Matthews (8)

although somewhat more complex. The FORTRAN language program consisting of the main program and subroutines for matrix inversion, matrix multiplication and matrix iteration are presented in Appendix B.

Accuracy of Computational Procedure

The formulation of the equations is such that the matrix which must be inverted approaches singularity as the half cone angle approaches zero. This is due to the fact that the equations of equilibrium, Eqs. (2.33) to (2.35), degenerate as α approaches zero and a limiting process must be utilized for the case $\alpha = 0$. In addition, for any reasonable length cone, the quantities s_1 and s_2 become very large as the cone angle is made small. Since differences of high powers of s_1 and s_2 are needed in the computation of the matrix coefficients, round-off errors and loss of significant figures degrade the results. As a consequence of these factors, computed frequencies and mode shapes for small cone angles are expected to be less accurate than those for larger cone angles.

Terms in the expressions for curvature, Eqs. (2.4) to (2.6), which are neglected in Eqs. (2.7) to (2.9) become less significant as α approaches 90° since the terms contain $\cos \alpha$. This fact also contributes to greater accuracy for the larger cone angles.

Second degree polynomials of the general form of Eqs. (4.1) to (4.3) were utilized for certain cases to determine the effect of choice of degree of the assumed longitudinal displacement polynomials upon the results. Differences between computed frequency parameters were found to increase as the circumferential wave number m is decreased and as the mode number is increased. For example, in a typical case, the difference in frequencies for the first mode is about two percent for $m=2$ and decreases to less than one-tenth of a percent at $m=9$, whereas, for the third mode the difference for $m=2$ is nine percent and decreases to one percent at $m=9$. Table I illustrates this point, wherein the results are normalized such that the frequencies determined utilizing the four term, third degree polynomials are equal to one, thereby allowing convenient comparison with frequencies determined from the use of the second degree polynomials.

As m increases, the complexity of the circumferential shape appears to compensate for the lack of accuracy in the longitudinal shape of the mode. That is, for the higher circumferential wave number shapes, the frequency is predominately determined by the complexity of the circumferential shape. The inaccuracy of the longitudinal shape does not seriously effect the natural frequencies of the lower modes. On the other hand, the

TABLE I

NORMALIZED FREQUENCIES FOR THREE AND FOUR TERM POLYNOMIALS

	<u>1st Mode</u>	<u>2nd Mode</u>	<u>3rd Mode</u>
m=2			
Three Term	102.2	105.4	108.9
Four Term	100.0	100.0	100.0
m=4			
Three Term	100.3	105.3	108.8
Four Term	100.0	100.0	100.0
m=9			
Three Term	100.03	100.05	101.0
Four Term	100.00	100.00	100.0

inability of the less complex (lower degree polynomial) longitudinal assumed shape to adequately represent the more complex modes is evident, i.e., the higher degree polynomial is better able to represent the higher modes, which is to be expected.

In this study, the primary interest is in the lower modes, especially the first and second. Therefore, it was decided to utilize the third degree polynomials as given by Eqs. (4.1) to (4.3) for the longitudinally varying displacement function. The use of higher degree polynomials would not significantly increase the accuracy of the frequencies and mode shapes of the first two modes, based upon results for the test case using both second and third degree polynomials.

According to Bolotin (1), convergence in connection with the Galerkin procedure has been investigated only in connection with very simple problems. The wide use of Galerkin's method for problems in which convergence is not conclusively proved is based upon a comparison of existing exact results with those obtained with Galerkin's method, for those few cases where exact solutions can be obtained analytically. One must rely to a certain extent on checks built into a computational procedure which may be designed to identify non-convergence. A check on mode orthogonality with respect to the generalized mass matrix was utilized in this study.

CHAPTER V

COMPARISON OF ANALYTICAL RESULTS WITH THE EXPERIMENTAL
DATA OF HU, GORMLEY, AND LINDHOLM

Geometry of the truncated conical shells taken from Ref. 6, and used here as comparative cases, is given in Table II. Parameters are as shown diagrammatically in Figure 2.1.

TABLE II

CONE GEOMETRY, CASES OF HU, GORMLEY, AND LINDHOLM

	Case 1	Case 2	Case 3	Case 4
Cone Half-Angle, α	14.24°	30.24°	45.12°	60.42°
Major Edge Radius, r_L	6.07 in.	7.95 in.	8.96 in.	10.00 in.
Minor Edge Radius, r_0	2.72 in.	3.49 in.	3.98 in.	4.45 in.
Length, L	13.2 in.	7.65 in.	4.96 in.	3.15 in.
Thickness, h	0.01 in.	0.01 in.	0.01 in.	0.01 in.
Completeness Parameter, s_2/s_1	2.23	2.28	2.24	2.25

Comparative results for Cases 1, 2, 3 and 4 are given by Tables III through VI. The frequency parameter Ω for these cases is defined by

$$\Omega = \omega r_L \left[\rho \frac{(1-\nu^2)}{E} \right]^{1/2} \quad (5.1)$$

Agreement between the theoretical and experimental data appears to improve as the cone angle increases. This trend is partially due to the fact that computational errors increase as the cone angle approaches zero, as explained in Chapter IV. In general, the agreement also improves in each case as m increases. Due to the low frequencies being measured, the experimental results, of course, were also subject to error. Errors introduced by cone imperfections, seams, supports, and method of excitation were most likely greater for the lower circumferential wave numbers.

It can be seen that the computer results agree quite well with the experimental data. It can also be noted from Tables III to VI that with few exceptions the theoretical frequencies are greater than the experimentally determined ones. Again this is to be expected because of the constraints imposed by an approximate method.

Mode shapes for Case 3 (45.12° cone half angle) are presented in Figures 5.1 and 5.2. Actually the normalized radial displacement is plotted rather than the

TABLE III
 FREQUENCY PARAMETERS, CASE 1

Circum-ferential Wave No.	Frequency Parameter Ω			
	1st Mode		2nd Mode	
	NASA-CR-384	Galerkin	NASA-CR-384	Galerkin
2	.00191	.00243	.0113	.0062
3	.00502	.00571	.0195	.0144
5	.0151	.01585	.0393	.0394
7	.0285	.0300	.0611	.0650
12	.0763	.0789	.112	.1285
18	.165	.169	-	.264

TABLE IV
 FREQUENCY PARAMETERS, CASE 2

Circum-ferential Wave No.	Frequency Parameter Ω			
	1st Mode		2nd Mode	
	NASA-CR-384	Galerkin	NASA-CR-384	Galerkin
2	.00151	.00191	-	.00578
3	.00422	.00456	-	.0128
5	.0122	.0126	-	.0333
7	.0242	.0244	.0626	.0627
12	.0647	.0656	.120	.129
18	.135	.1356	.200	.213

TABLE V
 FREQUENCY PARAMETERS, CASE 3

Circum-ferential Wave No.	Frequency Parameter Ω			
	1st Mode		2nd Mode	
	NASA-CR-384	Galerkin	NASA-CR-384	Galerkin
2	.00147	.00169	-	.00612
3	.00399	.00413	-	.0130
5	.0113	.01145	-	.0313
7	.0218	.0221	.0583	.0578
12	.0599	.0607	.127	.133
18	.123	.124	.187	.212

TABLE VI
 FREQUENCY PARAMETERS, CASE 4

Circum-ferential Wave No.	Frequency Parameter Ω			
	1st Mode		2nd Mode	
	NASA-CR-384	Galerkin	NASA-CR-384	Galerkin
2	.00139	.00144	-	.00663
3	.00377	.00367	-	.0133
5	.0104	.0104	-	.0298
7	.0200	.0200	.0573	.0533
12	.0552	.0548	.123	.1245
18	.113	.1125	.187	.196

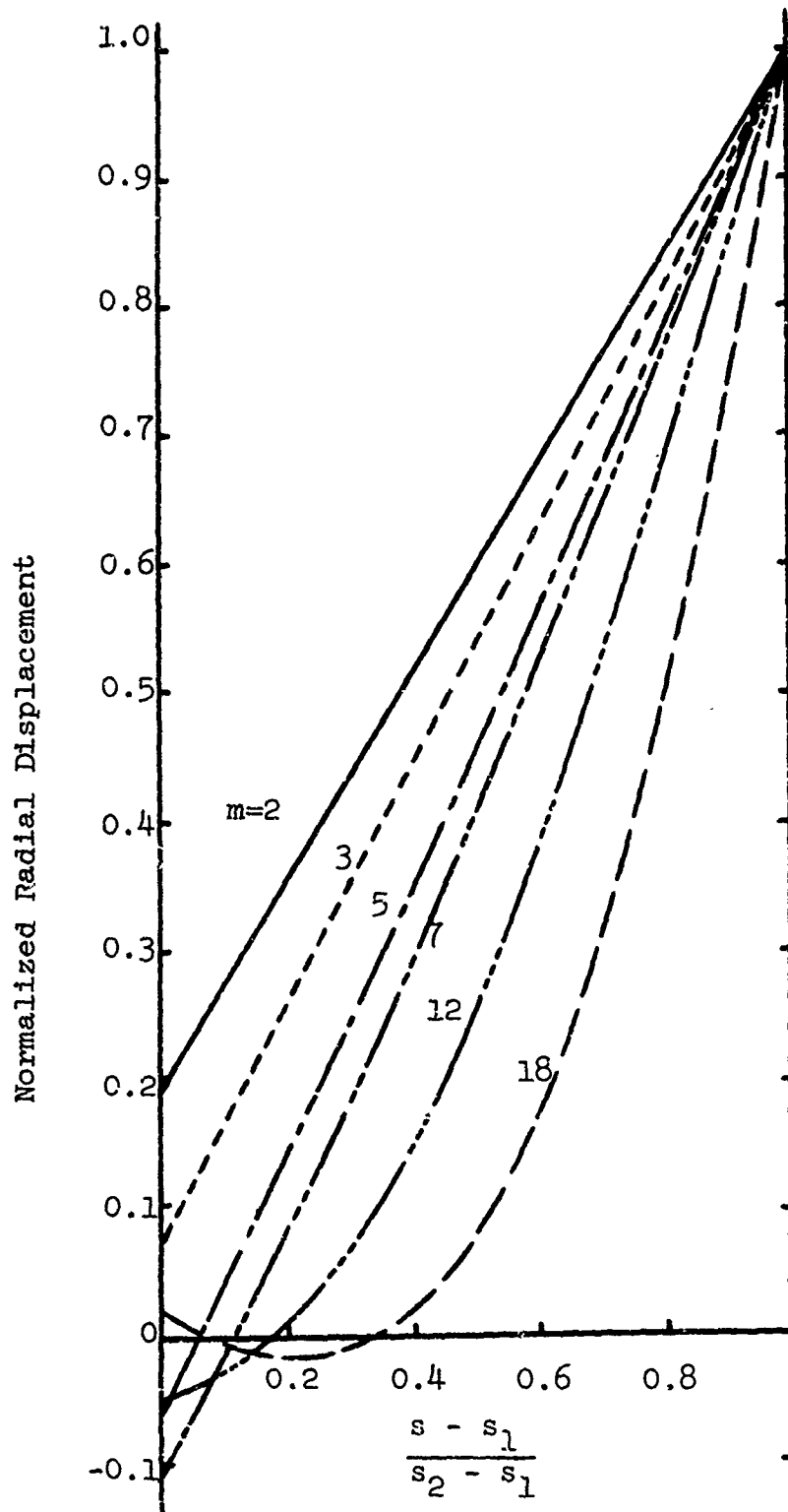


Figure 5.1 First Mode Radial Displacement Shapes, Case 3

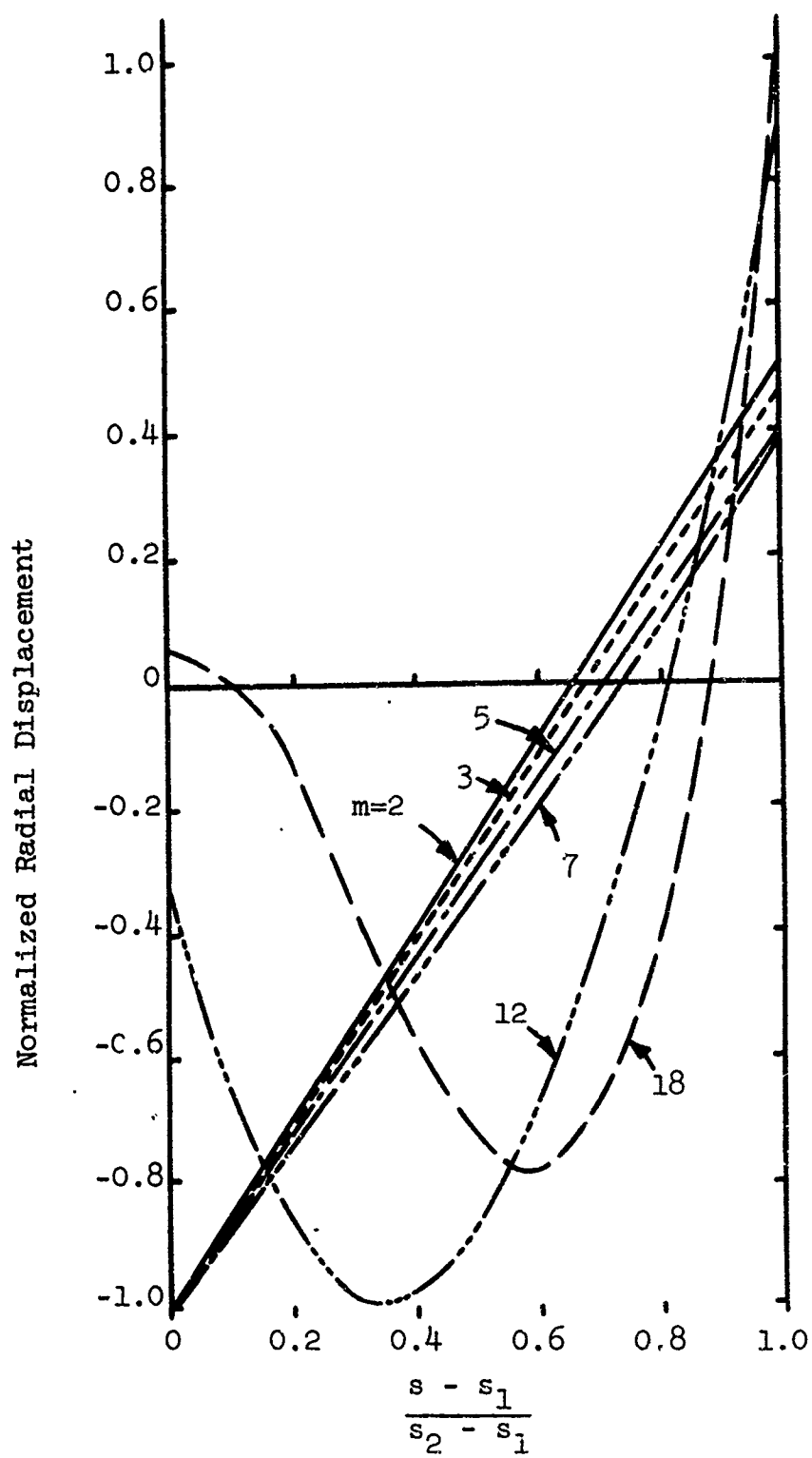


Figure 5.2 Second Mode Radial Displacement Shapes, Case 3

total displacement. Since the radial displacement is dominant for the first two modes, it was chosen for discussion purposes. Hereafter the expression "mode shape" is taken to mean the normalized radial displacement shape when reference is made to the figures. In general, the results agree favorably with those found experimentally by Hu and presented in Ref. 6. Figure 5.3 shows a comparison of the experimental and theoretical mode shapes for the first and second modes of Case 3 for $m=12$.

In Ref. 6, Hu, et al., propose the following semi-empirical frequency equation for thin free-free conical shells:

$$\Omega = \frac{h^2}{12 r_L^2} \frac{m(m-1)}{\sqrt{m^2 + 1}} (m + 1 + 4 \sin \frac{3\alpha}{2}) \quad (5.2)$$

It was shown that agreement between the experimentally determined frequency parameter and that given by Eq. (5.2) was in general very good for the range of parameters tested. It was also stated that the range of applicability of Eq. (5.2) with regard to the completeness parameter s_2/s_1 is uncertain. Equation (5.2) was developed to compare with experimental results having a completeness parameter of approximately 2.25.

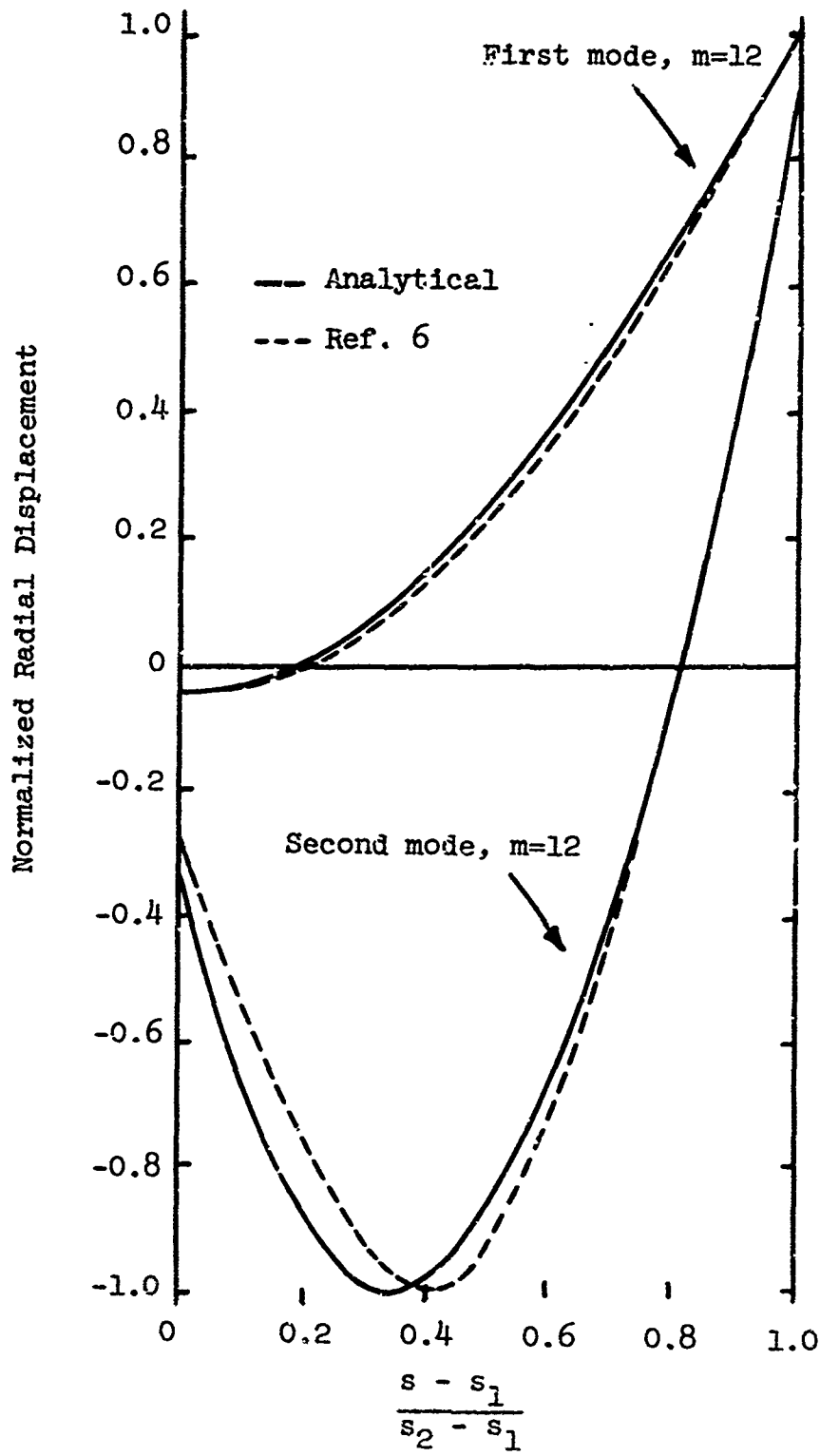


Figure 5.3 Comparison of Shapes

In order to determine the effect of completeness parameter upon frequency parameter, the basic shell of Case 3 was utilized, varying s_2 while holding s_1 constant. Results of varying s_2/s_1 from 1.1 to 10 are presented in Figure 5.4. It can be seen that for $m=6$ and above, the total variation in frequency parameter, for the range of s_2/s_1 considered, is almost constant. This means that the effect of completeness parameter becomes less pronounced as m increases, as one might suspect. For example, the approximate percentage increase in frequency parameter from $s_2/s_1 = 1.1$ to $s_2/s_1 = 10$ for $m=6$ is 65 percent while at $m=12$ it is only 20 percent. It should also be noted that the variation in frequency parameter between $s_2/s_1 = 1.5$ and $s_2/s_1 = 10$ amounts to about half of the total variation for the range of s_2/s_1 considered. Since the $s_2/s_1 = 2.25$ curve very nearly divides the area between the $s_2/s_1 = 1.5$ and $s_2/s_1 = 10$ curves, reasonably good results can be expected of Eq. (5.2) for very thin shells having a completeness parameter between 1.5 and 10, especially for the larger values of m .

Attempts were made to incorporate the completeness parameter s_2/s_1 into Eq. (5.2), thereby extending its range of applicability. However, these attempts were unsuccessful. A complete parametric study on completeness parameter and its effect in relation to cone angle,

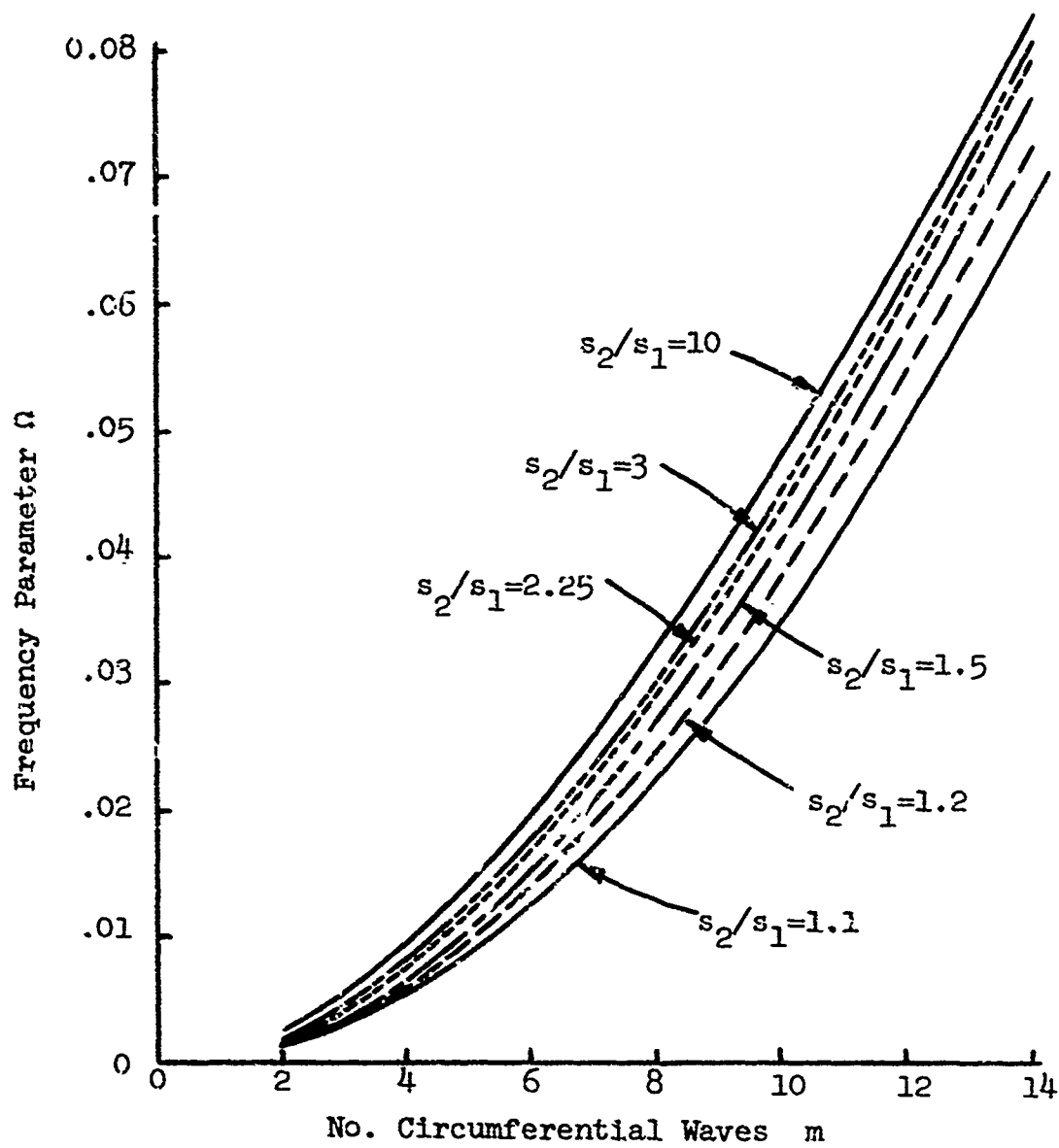


Figure 5.4 Effect of Varying Completeness Parameter

thickness, and other variables, is beyond the scope of this study.

CHAPTER VI

COMPARISON OF ANALYTICAL RESULTS WITH THE EXPERIMENTAL DATA OF WATKINS AND CLARY

The phenomenon wherein a different number of circumferential waves are present at the two cone edges in an apparent natural mode was observed by Watkins and Clary (12) but not by Hu, Gormley, and Lindholm (data used in Chapter V). As was mentioned in Chapter I, the validity of the experimental results of Watkins and Clary was questioned by Hu (5). Hu points out the care that must be exercised in setting up such an experiment in order to excite only the true natural modes of the cone. A reasonable theory which explains the results observed by Watkins and Clary, based upon theoretical frequencies and mode shapes, is presented in this chapter.

Geometry of the conical shells taken from Ref. 12 and used here as comparative cases are given by Table VII.

Comparative results for Cases 5, 6, 7, and 8 are shown by Figures 6.1 through 6.4. The frequency parameter $\Delta^{1/2}$ plotted in these figures is defined as

$$\Delta^{1/2} = \omega \lambda L (\rho (1 - \nu^2) / E)^{1/2} \quad (6.1)$$

TABLE VII

CONE GEOMETRY, CASES OF WATKINS AND CLARY

	Case 5	Case 6	Case 7	Case 8
Cone Half-Angle, α	3.18 ^o	7.59 ^o	14.04 ^o	23.96
Major Edge Radius, r_L	14.0"	14.0"	14.0"	14.0"
Minor Edge Radius, r_o	12.0"	10.0"	8.0"	6.0"
Length, L	36.0"	30.0"	24.0"	18.0"
Thickness, h	0.007"	0.007"	0.007"	0.007"
Completeness Parameter s_2/s_1	1.16	1.40	2.33	1.75

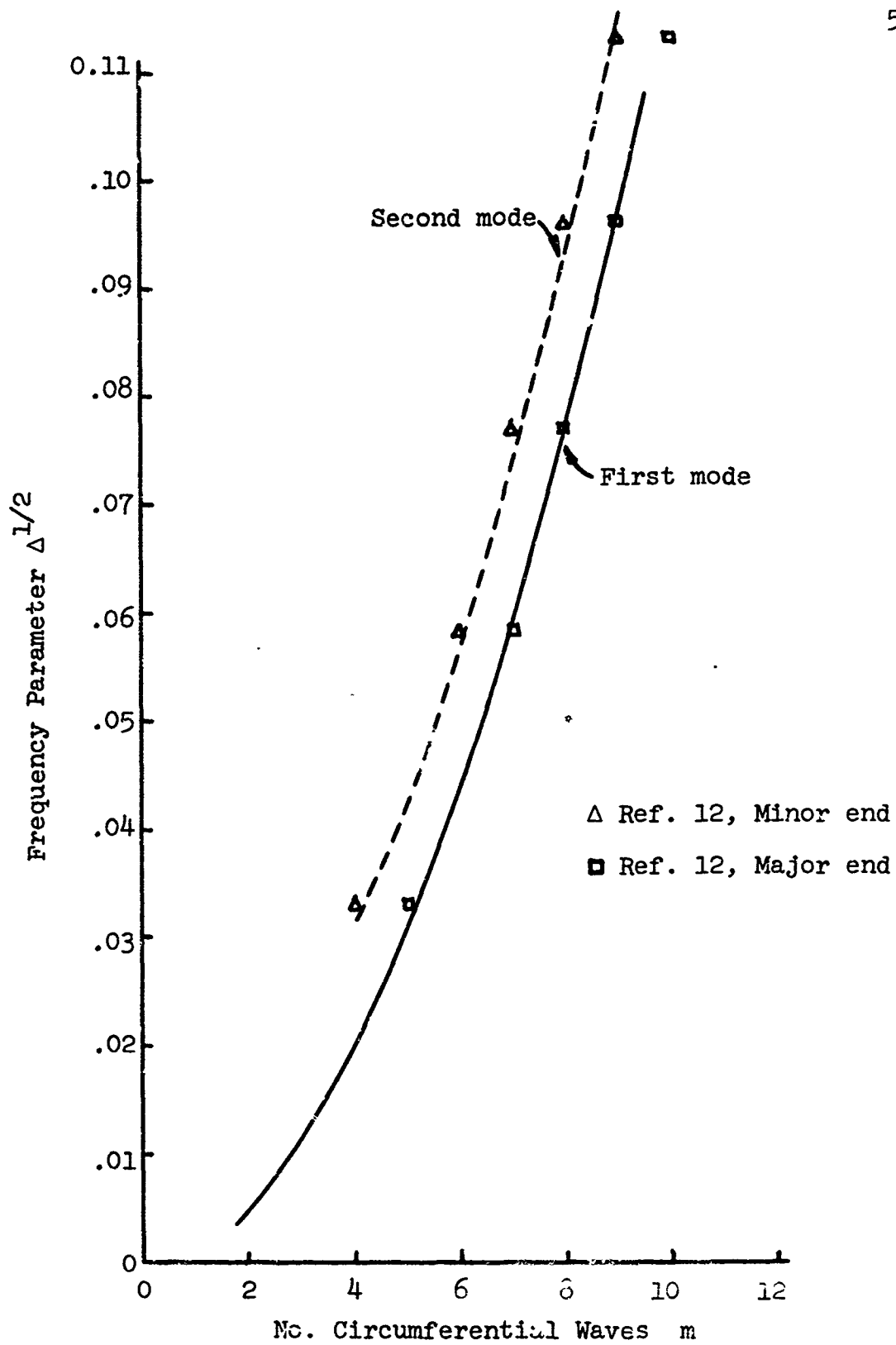


Figure 6.1 Frequency Parameter, Case 5

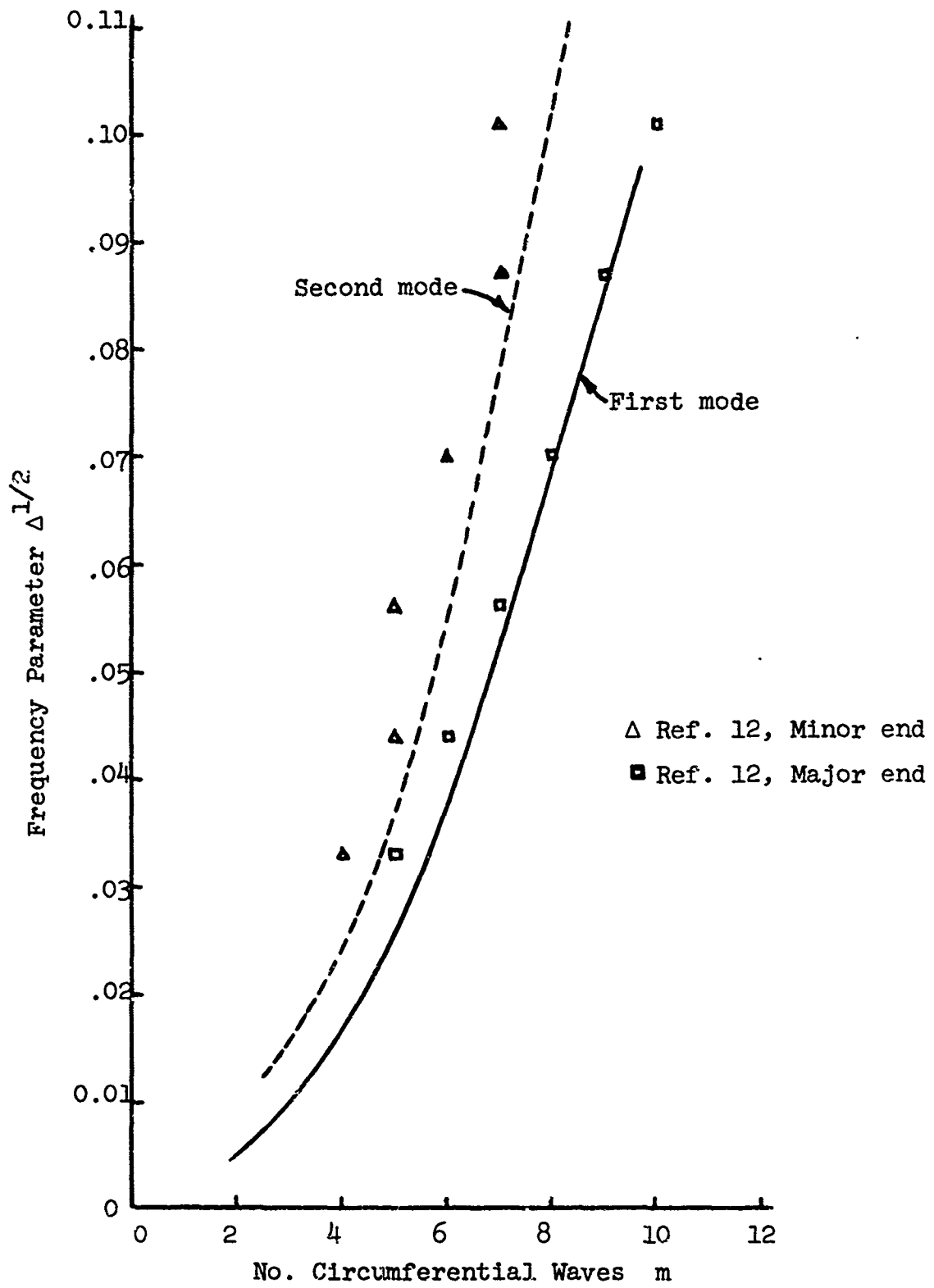


Figure 6.2 Frequency Parameter, Case 6

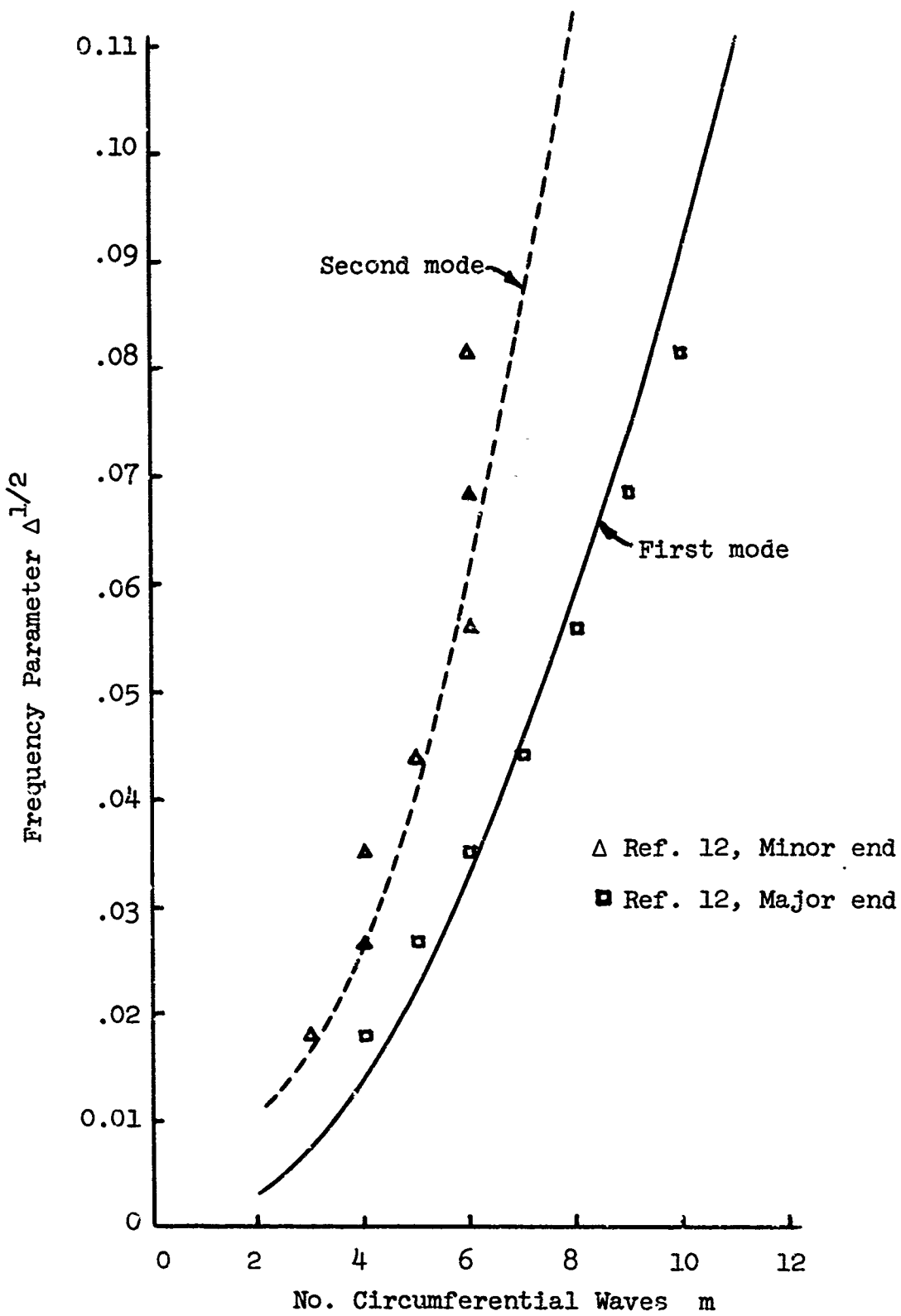


Figure 6.3 Frequency Parameter, Case 7

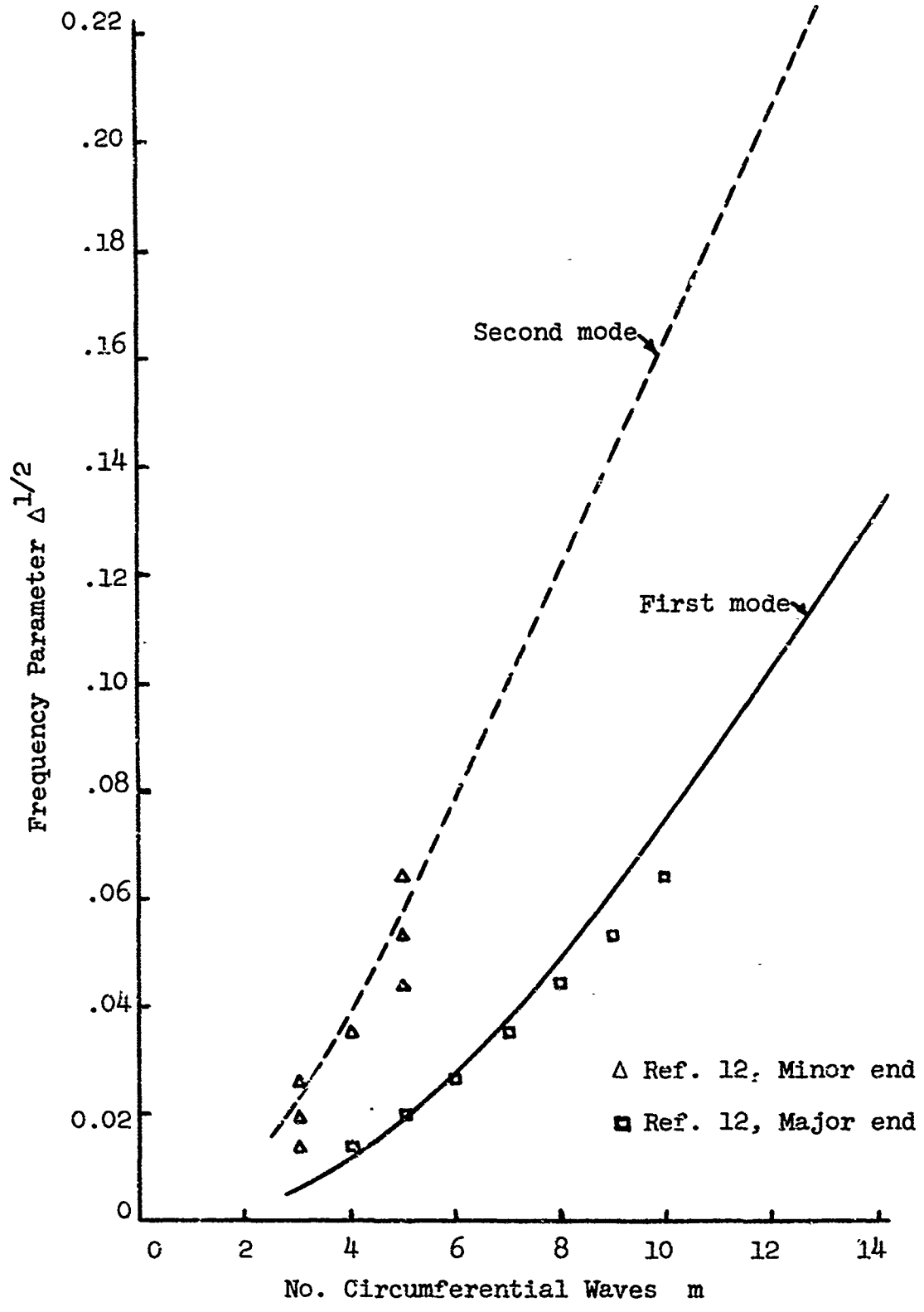


Figure 6.4 Frequency Parameter, Case 8

where λ is L/r_0 . This is the parameter used by Watkins and Clary. It can be seen that the first mode results compare favorably with the experimental data when the circumferential wave number observed by Watkins and Clary at the major (large) end is used. The semi-empirical equation proposed by Hu, et al., (6) also compares favorably to the Watkins and Clary data points associated with the circumferential wave number at the major edge. On the other hand, the data which corresponds to the circumferential wave number observed at the minor (small) end of the cone correlate reasonably well with the second analytically computed mode. This fact supports the theory that the experimental phenomenon observed by Watkins and Clary, wherein a different number of nodes were observed at the two cone edges, may have actually been a combination of the natural first and second mode shapes corresponding to different circumferential wave numbers.

In support of the above theory, it was noted from the computed data that the predominant displacement of the first mode occurs at the large end of the cone, whereas, the predominant displacement of the second mode occurs at the opposite edge. Consider, for example, the cone of Case 8. Experimentally it was observed that one mode had three circumferential waves at the minor edge and five waves at the major edge. The computed frequency parameter

for $m=3$, second mode, is $\Delta^{1/2} = 0.0180$ and for $m=5$, first mode, is $\Delta^{1/2} = 0.0195$. The corresponding mode shapes are presented in Figure 6.5. Note that the predominant displacements are as indicated above. The closeness of the frequencies and the shapes of the true natural modes, therefore, support the theory that these two modes could easily have been excited together in the experimental case with the observed results that three circumferential waves would appear at the small end of the cone while five waves would appear at the large end. Many other similar examples are evident from the data such as in Case 7 where for $m=5$, the second mode could have easily been excited with the first mode for $m=7$. In this case, computed frequency parameters are 0.0443 and 0.0450, respectively. The corresponding mode shapes are similar to those presented in Figure 6.5.

It can be shown that for certain combinations of circumferential wave numbers, coupling of the theoretical modes is possible as a result of the six point string suspension system utilized in the experiments. This analysis is given in Appendix C. However, only two specific modes of the many observed by Watkins and Clary fall into this category. Therefore, coupling due to the suspension is of minor importance and does not alter the validity of the previous discussion. The presence of the

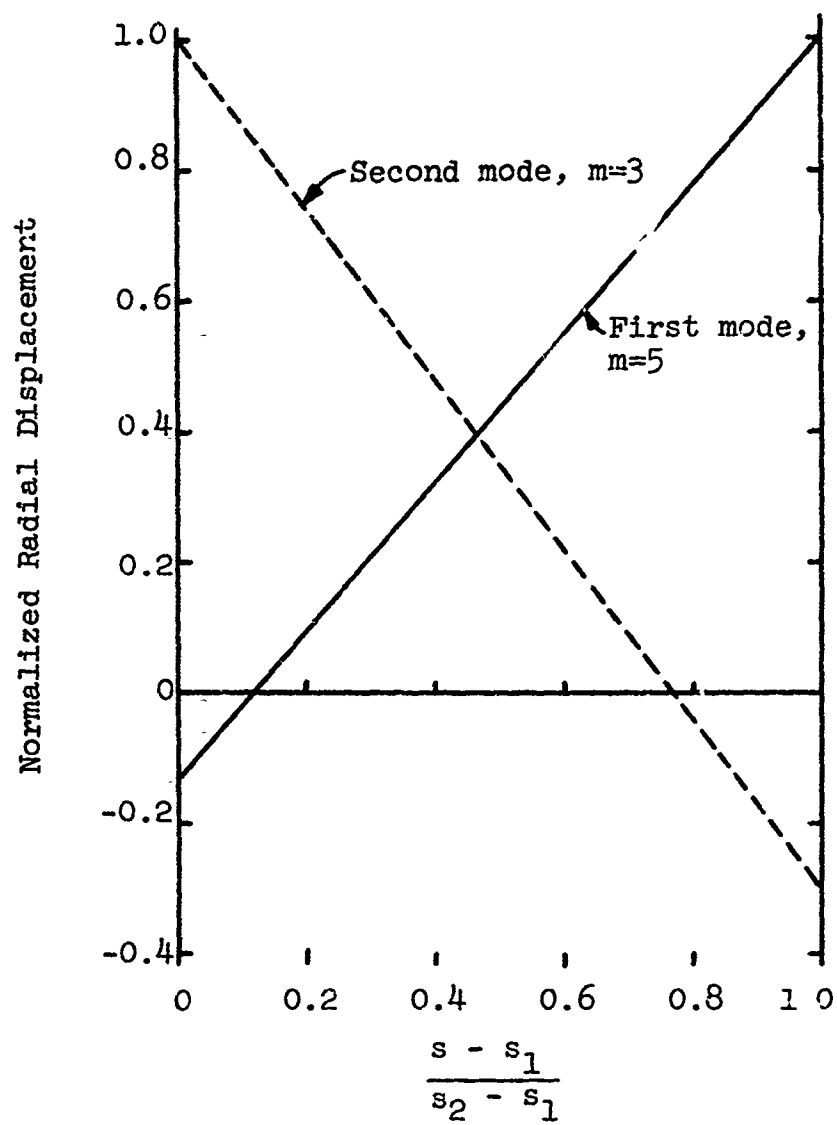


Figure 6.5 Normalized Radial Displacements, Case 8

suspension also has a minor numerical effect on the values of the frequencies except in the few cases where the suspension and nodal points coincide.

Due to the fact that the experimental frequency data plotted in Figures 6.1 through 6.4 correspond to complex mode shapes, whereas, the theoretical frequencies represent pure modes having the same number of nodes at both edges, comparisons of the data, other than those already made, are difficult. Since the mode shapes are so drastically different, conclusions regarding a comparison of frequencies would not be entirely valid.

CHAPTER VII

CONCLUSIONS

The results of this investigation have added credibility to the experimental data of Hu, Gormley, and Lindholm, and offered a plausible explanation to the phenomenon observed by Watkins and Clary. This phenomenon, wherein different numbers of nodes were observed at the two cone edges, was most likely caused by the combination of a fundamental mode, having a given number of circumferential waves, with a higher (second) mode having a smaller number of nodes. This is evidenced by the closeness of the respective frequencies and the location of the relative predominant displacements. Other possible causes for the observed complex mode shapes include material nonlinearities such as might be caused by non-constant shell thickness or seams, material or acoustic damping, and, in a few instances, coupling due to the manner of suspension. These, however, are believed to be of minor importance.

Results of the higher modes (not all presented here) could be improved considerably by adding more terms to the assumed polynomial displacement functions. This

may also require the use of double precision techniques in the computer inversion of the stiffness matrix since the accuracy of the matrix inversion decreases as the order of the matrix is increased. More sophisticated functions could also be used. However, the integration required to determine the matrix elements may then become unwieldy.

Use of the more general Flugge equations given in Appendix A would not have significantly affected the results of this study since the terms omitted in the Donnell type equations utilized here are of higher order for the very thin shells which were considered. For shells having the quantity $h/(s \sin \alpha)$ greater than $1/30$, it is recommended that the more general equations be used. The thin shell assumption $h/(s \sin \alpha) \ll 1$ was certainly satisfied since this quantity varied between $1/272$ and $1/2000$ for the eight cases discussed.

Based upon comparisons with available experimental data, it has been demonstrated that the modified Galerkin procedure can be utilized to determine the frequencies and mode shapes of a thin conical shell with free edges. The assumed displacement functions were found to adequately represent the motion of the shells considered, at least for the determination of the lower modes. A logical extension of this work would be to consider the vibrations

of the conical shell with other boundary conditions, some of which have not been investigated. The same general procedure could be used.

APPENDIX A

COMPLETE FLUGGE EQUATIONS

The equations presented in this appendix were derived from Flugge's (3) fundamental equations for a conical shell, which are valid for a variable wall thickness. His equations were modified by 1) restricting the equations to shells having a constant thickness, 2) adding inertia terms, and 3) changing the nomenclature to agree with that used in this study. The equations are based upon the assumptions that the displacements are small and that normals to the middle surface are preserved as such during deformation. The additional terms in the following equations which are not found in Eqs. (2.33) to (2.35) basically represent the influence of change in curvature on the normal and shearing forces and the influence of middle surface strains on the moments. For very thin shells these terms are of minor importance and consequently the simplified equations were used in this study.

$$\begin{aligned}
& D\left[\frac{(1+\nu)v' \csc \alpha}{2s} - \frac{(3-\nu)v' \csc \alpha}{2s^2} + u'' + \frac{(1-\nu)u' \csc^2 \alpha}{2s^2}\right. \\
& \left. + \frac{u'}{s} - \frac{u}{s^2} - \frac{vw' \cot \alpha}{s} + \frac{w \cot \alpha}{s^2}\right] + \frac{Dh^2}{12} \left[\frac{(1-\nu)u' \cot \alpha \csc^2 \alpha}{2s^4}\right. \\
& \left. - \frac{u \cot \alpha}{s^4} + \frac{w'''}{s} - \frac{(1-\nu)w'' \csc^2 \alpha}{2s^3} + \frac{(3-\nu)w' \csc^2 \alpha}{2s^4}\right. \\
& \left. + \frac{w'}{s^3} + \frac{w \cot^2 \alpha}{s^4}\right] \cot \alpha - \rho h \frac{\partial^2 u}{\partial t^2} = 0 \quad (A.1)
\end{aligned}$$

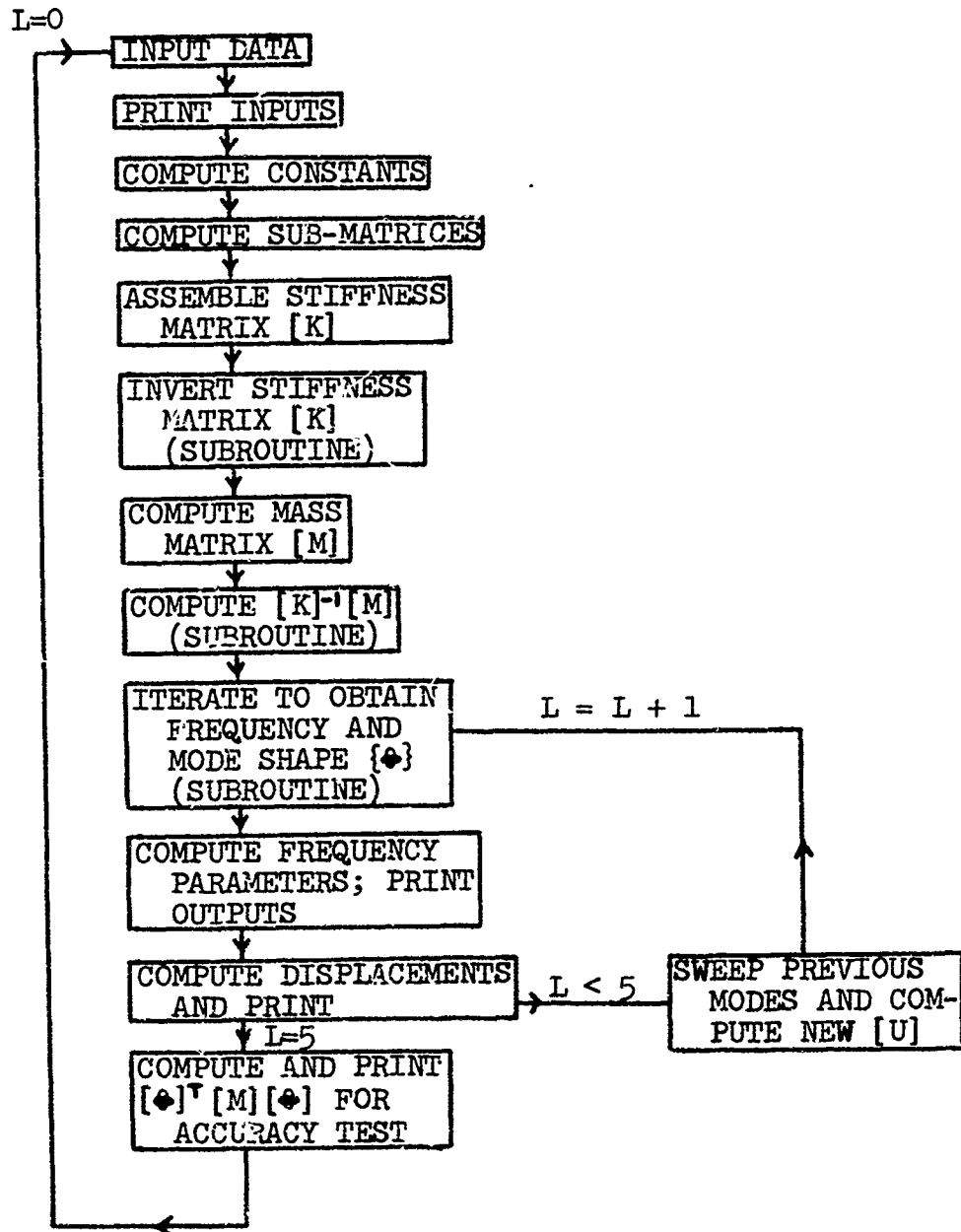
$$\begin{aligned}
& D\left[\frac{(1-\nu)v''}{2} + \frac{v' \csc^2 \alpha}{s^2} + \frac{(1-\nu)v'}{2s} - \frac{(1-\nu)v}{2s^2}\right. \\
& \left. + \frac{(1-\nu)u' \csc \alpha}{2s} + \frac{(3-\nu)u' \csc \alpha}{2s^2} - \frac{w' \cot \alpha \csc \alpha}{s^2}\right] \\
& + \frac{Dh^2}{12} \left[\frac{3(1-\nu)v'' \cot \alpha}{2s^2} - \frac{3(1-\nu)v' \cot \alpha}{2s^3} + \frac{3(1-\nu)v \cot \alpha}{2s^4}\right. \\
& \left. + \frac{(3-\nu)w'' \csc \alpha}{2s^2} - \frac{3(1-\nu)w' \csc \alpha}{2s^3} + \frac{3(1-\nu)w \csc \alpha}{2s^4}\right. \\
& \left. - \rho h \frac{\partial^2 v}{\partial t^2} = 0 \quad (A.2)
\end{aligned}$$

$$\begin{aligned}
& D\left[\frac{v \cdot \csc \alpha}{s^2} + \frac{vu'}{s} + \frac{u}{s^2} - \frac{w \cot \alpha}{s^2}\right] \cot \alpha + \frac{Dh^2}{12} \left[\frac{-(3-v)v'' \cdot \csc \alpha}{2s^2}\right. \\
& + \frac{(3-v)v' \cdot \csc \alpha}{2s^3} - \frac{(3+v)v \cdot \csc \alpha}{2s^4} - \frac{u'''}{s} + \frac{(1-v)u' \cdot \csc^2 \alpha}{2s^3} \\
& + \left.\frac{(1-v)u \cdot \csc^2 \alpha}{2s^4} - \frac{u' \cot \alpha}{s^3} + \frac{u(2+\cot^2 \alpha)}{s^4}\right] \cot \alpha \\
& - \frac{Dh^2}{12} \left[w'''' + \frac{2w'' \cdot \csc^2 \alpha}{s^2} + \frac{w \cdot \csc^4 \alpha}{s^4} + \frac{2w'''}{s} - \frac{2w' \cdot \csc^2 \alpha}{s^3}\right. \\
& - \frac{w''}{s^2} + \frac{2w \cdot \cot^2 \alpha \csc^2 \alpha}{s^4} + \frac{4w \cdot \csc^2 \alpha}{s^4} + \frac{w'}{s^3} \\
& \left. + \frac{w(2+\cot^2 \alpha) \cot^2 \alpha}{s^4}\right] - \rho h \frac{\partial^2 w}{\partial t^2} = 0 \tag{A.3}
\end{aligned}$$

APPENDIX B

FORTRAN COMPUTER PROGRAM

FLOW DIAGRAM: CONICAL SHELL VIBRATION COMPUTER PROGRAM



COMPUTER PROGRAM NOMENCLATURE

ALPHA	= α (half cone angle)	
CW, M	= m (no. circumferential waves)	
DISP	= displacements	
E	= E (Young's Modulus)	
FPAR	= frequency parameter $\Delta^{1/2}$	
FPAR2	= frequency parameter Ω	
H	= h (thickness)	
L	= count on modes	
OMEGA	= frequency	
PHI	= mode shape	
RHO	= ρ (density)	
RL	= r_L	} Defined by Figure 2.1
RO	= r_o	
S	= s	
S1	= s_1	
S2	= s_2	
SM1 to SM2	= submatrices used to generate XK and XM	
V1 to V-32	= various combinations of s_1, s_2, ν, α , etc., which are used repeatedly	
XK	= stiffness of matrix	
XKI	= inverse of stiffness matrix	
XLEN	= L(length)	
XM	= mass matrix	
XMU	= ν (Poisson's ratio)	
XT	= $k (h^2/12)$	

```

C   THE PURPOSE OF THIS PROGRAM IS THE SOLUTION OF MULTI-DEGREE
C   OF FREEDOM VIBRATIONS PROBLEMS FOR THE NATURAL FREQUENCIES
C   AND MODE SHAPES BY ITERATIVE METHODS.
C   BASIC EQUATIONS  $1./(\Omega^2)*A=XKI*M*A$ 
C   WHERE A ON THE RIGHT IS A TRIAL EIGENVECTOR
C   XKI IS THE INVERSE OF THE STIFFNESS MATRIX
C   M IS THE MASS MATRIX
C   A ON THE LEFT IS THE UNITIZED RESULT
C   SIZES  $XK=M*M$   $XM=M*M$   $A=M*I$ 
C   DIMENSION XK(21,21),XKI(21,21),U(21,21),UQ(21,21),XM(21,21),C(21,1)
C   1,PHI(21,21),PHIT(21,21),SM1(4,4),SM2(4,4),SM3(4,4),SM4(4,4),
C   2SM5(4,4),SM6(4,4),SM7(4,4),SM8(4,4),SM9(4,4),SM10(4,4),SM11(4,4)
C   DIMENSION ROW(21,21),DISP(21,21)
100 FORMAT(1H1,4X,18HENTER NEW DATA SET.//)
101 FORMAT(I2)
102 FORMAT(10X,2HM=,I2)
103 FORMAT(8F10.0)
107 FORMAT(10X,11HMODE SHAPE ,I2,5X,2HO ,I2,1PE15.7)
108 FORMAT(10X,6HOMEGA ,I2,1PE20.7)
109 FORMAT(5X,14HEND OF PROBLEM)
110 FORMAT(//)
111 FORMAT (10X,26HORTHOGONALIZED MASS MATRIX,2I2,1PE15.7)
113 FORMAT(10X,19HFREQUENCY PARAMETER,1PE15.7)
114 FORMAT(1HO,10X,44HFREQUENCIES AND MODE SHAPES OF CONICAL SHELL)
115 FORMAT(1X,1P4E17.7)
116 FORMAT(10X,6HLENGTH,10X,9HTHICKNESS,8X,9HNO. WAVES,12X,1HE)
117 FORMAT(10X,2HS1,15X,2HS2,13X,5HALPHA)
118 FORMAT(10X,2HRO,15X,2HRL,15X,3HRHO,14X,3HXMU)
120 FORMAT(10X,4HS/S2,14X,1HU,15X,1HV,15X,1HW)
C   READ INPUT DATA AND COMPUTE XKI
C   INPUT DATA
C   PRINT 114
1   READ 101,M
C   PRINT 100
C   L=0
C   NOTE=1
C   PRINT 102,M
C   PRINT 110
2   READ 103,RO,RL,RHO,XMU,XLEN,H,CW,E
C   PRINT 110
C   PI=3.1415927
C   ALPHA=ATANF((RL-RO)/XLEN)
C   S1=RO/SINF(ALPHA)
C   S2=RL/SINF(ALPHA)
C   ALPD=ALPHA*57.29578
C   XLAM=XLEN/RO
C   PRINT 113
C   PRINT 115,RO,RL,RHO,XMU
C   PRINT 116
C   PRINT 115,XLEN,H,CW,E
C   PRINT 117
C   PRINT 115,S1,S2,ALPD
C   PRINT 110
C   XT=(H*H)/12.0
C   COMPUTE CONSTANT VALUES

```

```

V1=S2-S1
V2=S2*S2-S1*S1
V3=S2**3-S1**3
V4=S2**4-S1**4
V5=S2**5-S1**5
V6=S2**6-S1**6
V7=LOGF(S2)-LOGF(S1)
V8=S2*S2
V9=S2**3
V10=S2**4
V11=CW/SINF(ALPHA)
V12=V1!*V11
V13=COSF(ALPHA)/SINF(ALPHA)
V14=V13*V13
V15=1.0+0.5*(1.0-XMU)*V12
V16=0.5*(1.0-XMU)+V12
V17=(XT*V12)*(V12-4.0)
V18=-(1.0-XMU)/2.0
V19=XT*(2.0*V12+1.0)
V20=-XT*V12*(3.0-XMU)
V21=-XT*XMU*V12
V22=XT*XMU
V23=1.0/S2-1.0/S1
V24=1.0/(S2*S2)-1.0/(S1*S1)
V25=V11*(3.0-XMU)/2.0
V26=-V11*(1.0+XMU)/4.0
V27=-V11*(1.0-3.0*XMU)/4.0
V28=(RHO*(1.0-XMU*XMU))/(E*386.088)
V29=S2**5
V30=S2**6
V31=S2**7-S1**7
V32=S2**8-S1**8
C COMPUTE SUBMATRICES
N=M/3
SM1(1,1)=V2/2.0
SM1(1,2)=V3/(3.0*S2)
SM1(1,3)=V4/(4.0*V8)
SM1(2,2)=SM1(1,3)
SM1(2,3)=V5/(5.0*V9)
SM1(3,3)=V6/(6.0*V10)
SM1(1,4)=SM1(2,3)
SM1(2,4)=SM1(3,3)
SM1(3,4)=V31/(7.0*V29)
SM1(4,4)=V32/(8.0*V30)
DO 200 I=1,N
DO 200 J=1,N
200 SM1(J,I)=SM1(I,J)
SM2(1,1)=V7
SM2(1,2)=V1/S2
SM2(1,3)=V2/(2.0*V8)
SM2(2,2)=SM2(1,3)
SM2(2,3)=V3/(3.0*V9)
SM2(3,3)=V4/(4.0*V10)
SM2(1,4)=SM2(2,3)
SM2(2,4)=SM2(3,3)
SM2(3,4)=V5/(5.0*V29)

```

```

SM2(4,4)=V6/(6.0*V30)
DO 210 I=1,N
DO 210 J=1,N
210 SM2(J,I)=SM2(I,J)
SM3(1,1)=0.0
SM3(1,2)=0.0
SM3(1,3)=0.0

```

```

SM3(2,2)=V2/(2.0*V8)
SM3(2,3)=(2.0*V3)/(3.0*V9)
SM3(3,3)=V4/V10
SM3(1,4)=0.0
SM3(2,4)=(3.0*V4)/(4.0*V10)
SM3(3,4)=(6.0*V5)/(5.0*V29)
SM3(4,4)=(3.0*V6)/(2.0*V30)

```

```

DO 220 I=1,N
DO 220 J=1,N
220 SM3(J,I)=SM3(I,J)
SM4(1,1)=-V24/2.0
SM4(1,2)=-V23/S2
SM4(1,3)=V7/V8
SM4(2,2)=SM4(1,3)
SM4(2,3)=V1/V9
SM4(3,3)=V2/(2.0*V10)
SM4(1,4)=SM4(2,3)
SM4(2,4)=SM4(3,3)
SM4(3,4)=V3/(3.0*V29)
SM4(4,4)=V4/(4.0*V30)

```

```

DO 230 I=1,N
DO 230 J=1,N
230 SM4(J,I)=SM4(I,J)
DO 240 I=1,N
DO 240 J=1,N
240 SM5(I,J)=0.0
SM5(3,3)=(2.0*V2)/V10
SM5(3,4)=(4.0*V3)/V29
SM5(4,3)=SM5(3,4)
SM5(4,4)=(9.0*V4)/V30
SM6(1,1)=0.0
SM6(1,2)=V1/S2
SM6(1,3)=V2/V8
SM6(2,2)=0.0
SM6(2,3)=V3/(3.0*V9)
SM6(3,3)=0.0
SM6(1,4)=V3/V9
SM6(2,4)=V4/(2.0*V10)
SM6(3,4)=V5/(5.0*V29)
SM6(4,4)=0.0
DO 250 I=1,N
DO 250 J=1,N
250 SM6(J,I)=-SM6(I,J)
SM7(1,1)=0.0
SM7(1,2)=0.0
SM7(1,3)=0.0
SM7(2,2)=V7/V8
SM7(2,3)=(2.0*V1)/V9
SM7(3,3)=(2.0*V2)/V10

```

```


```

```


```

```


```

```


```

```

SM7(1,4)=0.0
SM7(2,4)=(3.0*V2)/(2.0*V10)
SM7(3,4)=(2.0*V3)/V29
SM7(4,4)=(9.0*V4)/(4.0*V30)
DO 260 I=1,N
DO 260 J=I,N
260 SM7(J,I)=SM7(I,J)
SM8(1,1)=0.0
SM8(1,2)=V1/S2
SM8(1,3)=V2/V8
SM8(2,2)=SM8(1,3)
SM8(2,3)=V3/V9
SM8(3,3)=V4/V10
SM8(1,4)=SM8(2,3)
SM8(2,4)=SM8(3,3)
SM8(3,4)=V5/V29
SM8(4,4)=V6/V30
DO 270 I=1,N
DO 270 J=I,N
270 SM8(J,I)=SM8(I,J)
SM9(1,1)=V24
SM9(1,2)=V23/S2
SM9(1,3)=0.0
SM9(2,2)=0.0
SM9(2,3)=V1/V9
SM9(3,3)=V2/V10
SM9(1,4)=SM9(2,3)
SM9(2,4)=SM9(3,3)
SM9(3,4)=V3/V29
SM9(4,4)=V4/V30
DO 280 I=1,N
DO 280 J=I,N
280 SM9(J,I)=SM9(I,J)
SM10(1,1)=0.0
SM10(1,2)=V23/S2
SM10(1,3)=0.0
SM10(2,2)=0.0
SM10(2,3)=(3.0*V1)/V9
SM10(3,3)=(4.0*V2)/V10
SM10(1,4)=(3.0*V1)/V9
SM10(2,4)=(4.0*V2)/V10
SM10(3,4)=(5.0*V3)/V29
SM10(4,4)=(6.0*V4)/V30
DO 290 I=1,N
DO 290 J=I,N
290 SM10(J,I)=SM10(I,J)
DO 300 I=1,N
DO 300 J=I,N
300 SM11(I,J)=0.0
SM11(2,3)=(2.0*V1)/V9
SM11(3,2)=SM11(2,3)
SM11(3,3)=(4.0*V2)/V10
SM11(2,4)=(3.0*V2)/V10
SM11(4,2)=SM11(2,4)
SM11(3,4)=(6.0*V3)/V29
SM11(4,3)=SM11(3,4)

```

```

SM11(4,4)=(9.0*V4)/V3C
C COMPUTE STIFFNESS MATRIX
C ALPHA-ALPHA SUBMATRIX
DO 310 I=1,N
DO 310 J=1,N
XK(I,J)=V15*SM2(I,J)+SM3(I,J)+XMU*SM8(I,J)
C BETA-BETA SUBMATRIX
IPN=I+N
JPN=J+N
XK(IPN,JPN)=V16*SM2(I,J)-V18*(SM3(I,J)-SM8(I,J))
C GAMMA-GAMMA SUBMATRIX
IP2N=I+2*N
JP2N=J+2*N
XK(IP2N,JP2N)=V14*SM2(I,J)+V17*SM4(I,J)
1+V19*SM7(I,J)+XT*SM5(I,J)+V20*SM9(I,J)+V21*SM10(I,J)
2+V22*SM11(I,J)
C ALPHA-BETA SUBMATRIX
XK(I,JPN)=V25*SM2(I,J)+V26*SM6(I,J)+V27*SM8(I,J)
C ALPHA-GAMMA SUBMATRIX
XK(I,JP2N)=V13*(-SM2(I,J)+(XMU/2.0)*(SM6(I,J)-SM8(I,J)))
C BETA-GAMMA SUBMATRIX
310 XK(IPN,JP2N)=-V11*V13*SM2(I,J)
DO 320 I=1,M
DO 320 J=1,M
320 XK(J,I)=XK(I,J)
CALL MAINV(XK,XKI,M)
CALL MAMUL(XKI,XK,U,M,M,M)
C COMPUTE MASS MATRIX
DO 350 I=1,N
DO 350 J=1,N
IPN=I+N
JPN=J+N
JP2N=J+2*N
IP2N=I+2*N
XM(I,J)=V28*SM1(I,J)
XM(IPN,JPN)=XM(I,J)
350 XM(IP2N,JP2N)=XM(I,J)
C COMPUTE U=XKI*XM
CALL MAMUL(XKI,XM,U,M,M,M)
C ITERATE
5 CALL ITER(U,Q,OMEGA,M,NOTE)
L=L+1
DO 10 I=1,M
PHI(I,L)=Q(I)
10 PHIT(L,I)=Q(I)
FPAR=SQRTF(((1.0-XMU*XMU)*RHO*XLAM*XLAM*XLEN*XLEN*OMEGA*OMEGA)
1/(E*386.088))
FPAR2=(FPAR*RL*RO)/(XLEN*XLEN)
PRINT 107,(L,I,Q(I),I=1,M)
PRINT 110
PRINT 108,L,OMEGA
PRINT 113,FPAR
PRINT 113,FPAR2
PRINT 110
59 DO 60 I=1,M
DO 60 J=1,3

```

```

60 ROW(J,I)=0.
   PRINT 120
   FL=S1/S2
   SINC=(S2-S1)/(20.0*S2)
62 ROW(1,1)=1.0
   ROW(1,2)=FL
   ROW(1,3)=FL*FL
   ROW(1,4)=FL*FL*FL
   ROW(2,5)=1.0
   ROW(2,6)=FL
   ROW(2,7)=ROW(1,3)
   ROW(2,8)=ROW(1,4)
   ROW(3,9)=1.0
   ROW(3,10)=FL
   ROW(3,11)=ROW(1,3)
   ROW(3,12)=ROW(1,4)
   CALL MAMUL(ROW,Q,DISP,3,M,1)
   PRINT 115,FL,DISP(1,1),DISP(2,1),DISP(3,1)
   FL=FL+SINC
   IF(FL-1.0)62,63,63
63 CONTINUE
   PRINT 110
   IF(L-5) 6,8,8
C   FORM NEW U=U-UO
   6 CALL MAMUL(XM,Q,UO,M,M,1)
   CALL MTMUL(Q,UO,XK,1,M,1)
   DEN=XK(1,1)*(OMEGA)**2
   CALL MTMUL(Q,XM,XK,1,M,M)
   CALL MAMUL(Q,XK,UO,M,1,M)
   DO 7 I=1,M
   DO 7 J=1,M
   UO(I,J)=UO(I,J)/DEN
   7 U(I,J)=U(I,J)-UO(I,J)
   AA=0.
   BB=C.
   DO 11 I=1,M
   AA=AA+1.
   11 BB=BB+O(I)
   IF (AA-BB) 5,12,5
   12 NOTE=2
   GO TO 5
C   FIND ORTHOGONALIZED MASS MATRIX TO TEST FOR ACCURACY
   8 CALL MAMUL(XM,PHI,XK,M,M,5)
   CALL MAMUL(PHIT,XK,XKI,5,M,5)
   PRINT 111,((I,J,XKI(I,J),I=1,5),J=1,5)
   PRINT 110
   PRINT 109
   GO TO 1
   END(1,0,0,0,0,0,1,0,0,1,0,0,0,0,0)

```

SUBROUTINE MAMJL (A,B,C,M,N,MM)

79

SUBROUTINE MAMUL (A,B,C,M,N,MM)

```
C THIS SUBROUTINE IS FOR THE COMPUTATION OF MATRIX C FROM C=A*B
C WHERE C IS AN M*MM MATRIX, A IS AN M*N, B IS AN N*MM
  DIMENSION A(21,21),B(21,21),C(21,21)
  DO 3 I=1,M
  DO 3 J=1,MM
  C(I,J)=0.
  DO 3 K=1,N
3 C(I,J)=C(I,J)+A(I,K)*B(K,J)
  RETURN
  END(1,0,0,0,0,0,C,1,0,0,1,0,0,0,0,0)
```

```
SUBROUTINE MTMUL(A,B,C,M,N,K)
```

```
SUBROUTINE MTMUL(A,B,C,M,N,K)  
DIMENSION A(21,1),B(21,21),C(21,21),AT(1,21)  
DO 1 I=1,N  
1 AT(1,I)=A(1,I)  
DO 2 I=1,K  
C(1,I)=0.  
DO 2 J=1,N  
2 C(1,I)=C(1,I)+AT(1,J)*B(J,I)  
RETURN  
END(1.0,0.0,0.0,0.1,0.0,0.1,0.0,0.0,0.0)
```

SUBROUTINE MAINV (A,AINV,M)

81

SUBROUTINE MAINV (A,AINV,M)

```

C THIS SUBROUTINE IS FOR COMPUTING MATRIX AINV WHICH IS THE
C INVERSE OF MATRIX A
DIMENSION A(21,21),B(21,42),AINV(21,21)
N = 2*M
DO 4 I=1,M
DO 5 J=1,M
B(I,J) = A(I,J)
5 CONTINUE
4 CONTINUE
L=M+1
DO 6 I=1,M
DO 7 J=L,N
IF (I-J+M) 8,9,8
8 B(I,J) = 0.
GO TO 7
9 B(I,J) = 1.
7 CONTINUE
6 CONTINUE
DO 10 J=1,M
C = B(J,J)
IF (C) 20,21,20
20 DO 11 K=1,N
11 B(J,K) = B(J,K) / C
DO 14 L=1,M
IF(L-J) 13,14,13
13 D = B(L,J)
DO 15 K=1,N
15 B(L,K) = B(L,K) - B(J,K) * D
14 CONTINUE
10 CONTINUE
L = M+1
DO 16 I=1,M
DO 17 J=1,M
L=M+J
AINV(I,J)=B(I,L)
17 CONTINUE
16 CONTINUE
GO TO 23
21 PRINT 22
22 FORMAT(///.5X,39HINVALID SOLUTION—ZERO DIVISOR IN MAINV.///)
23 RETURN
END(1,C,C,0,0,C,1,C,0,1,0,0,0,0,0)

```

SUBROUTINE ITER (U,Q,OMEGA,M,NOTE)

82

```
SUBROUTINE ITER (U,Q,OMEGA,M,NOTE)
DIMENSION U(21,21),Q(21,1),A(21,1)
X=0.
DO 1 I=1,M
1 Q(I)=1.
GO TO (3,7),NOTE
7 DO 8 I=1,M.2
8 Q(I)=-1.
3 CALL MAMUL(U,Q,A,M,M,1)
RO=A(M)
B=0.
DO 6 I=1,M
6 B=B+Q(I)
C=0.
DO 4 I=1,M
4 C=C+Q(I)
X=X+1.
IF(X-100.) 10,10,5
10 IF (ABS(B-C)-.0000001) 5,5,3
5 PRINT 300,X
IF(RO)11,12,12
11 PRINT 301,RO
12 RO=ABS(RO)
OMEGA=SQRT(1./RO)
300 FORMAT (10X,21HNUMBER OF ITERATIONS .1PE15.7,/)
301 FORMAT (10X,14HOMEGA NEGATIVE .1PE15.7,/)
RETURN
END(1,0,0,0,0,C,1,C,0,1,0,0,0,0,0)
```

APPENDIX C

COUPLING OF MODES

A mathematical demonstration that the natural modes of the conical shell are coupled by the six-point string suspension utilized by Watkins and Clary is presented in this appendix.

In the expansion of the kinetic energy expression

$$T = 1/2 \iint \rho h (\dot{u}^2 + \dot{v}^2 + \dot{w}^2) s \sin \alpha \, ds d\theta \quad (C.1)$$

the cross terms involving m and n , two distinct modes, integrate to zero, verifying that no inertial coupling exists. Elastic coupling due to the presence of the strings will now be examined. Consider the six support strings to be located at $\theta=0, \pi/3, 2\pi/3, 4\pi/3$ and $5\pi/3$. The displacement of the strings in the m^{th} mode is longitudinal only and is given by

$$u_1 = \varphi_{u_m} \quad q_1 = \alpha_m(s) \cos m\theta \cdot q_1 \quad (c.2)$$

$$u_2 = \varphi_{u_m} \quad q_2 = \alpha_m(s) \sin m\theta \cdot q_2 \quad (C.3)$$

The two functions are needed for complete generality in orientation of the mode with respect to the support strings.

The total displacement in the direction of the suspension strings is then

$$u = u_1 + u_2 \quad (C.4)$$

Forces in the strings are given by Eqs. (C.5) to (C.10) where k represents here the string spring constant.

$$\theta = 0: -ku_1 - ku_2 = -k\alpha_m(s)[\cos 0 \cdot q_1 + \sin 0 \cdot q_2] \quad (C.5)$$

$$\theta = \pi/3: -ku_1 - ku_2 = -k\alpha_m(s)[\cos \pi/3 \cdot q_1 + \sin \pi/3 \cdot q_2] \quad (C.6)$$

$$\theta = 2\pi/3: -ku_1 - ku_2 = -k\alpha_m(s)[\cos 2\pi/3 \cdot q_1 + \sin 2\pi/3 \cdot q_2] \quad (C.7)$$

$$\theta = \pi: -ku_1 - ku_2 = -k\alpha_m(s)[\cos \pi \cdot q_1 + \sin \pi \cdot q_2] \quad (C.8)$$

$$\theta = 4\pi/3: -ku_1 - ku_2 = -k\alpha_m(s)[\cos 4\pi/3 \cdot q_1 + \sin 4\pi/3 \cdot q_2] \quad (C.9)$$

$$\theta = 5\pi/3: -ku_1 - ku_2 = -k\alpha_m(s)[\cos 5\pi/3 \cdot q_1 + \sin 5\pi/3 \cdot q_2] \quad (C.10)$$

A virtual displacement in the n^{th} mode is given by Eqs. (C.11) to (C.16).

$$\theta = 0: \delta u_1 + \delta u_2 = \alpha_n(s)[\cos 0 \cdot \delta q_3 + \sin 0 \cdot \delta q_4] \quad (C.11)$$

$$\theta = \pi/3: \delta u_1 + \delta u_2 = \alpha_n(s)[\cos \pi/3 \cdot \delta q_3 + \sin \pi/3 \cdot \delta q_4] \quad (C.12)$$

$$\theta = 2\pi/3: \delta u_1 + \delta u_2 = \alpha_n(s)[\cos 2n\pi/3 \cdot \delta q_3 + \sin 2n\pi/3 \cdot \delta q_4] \quad (C.13)$$

$$\theta = \pi: \delta u_1 + \delta u_2 = \alpha_n(s)[\cos n\pi \cdot \delta q_3 + \sin n\pi \cdot \delta q_4] \quad (C.14)$$

$$\theta = 4\pi/3: \delta u_1 + \delta u_2 = \alpha_n(s)[\cos 4n\pi/3 \cdot \delta q_3 + \sin 4n\pi/3 \cdot \delta q_4] \quad (C.15)$$

$$\theta = 5\pi/3: \delta u_1 + \delta u_2 = \alpha_n(s)[\cos 5n\pi/3 \cdot \delta q_3 + \sin 5n\pi/3 \cdot \delta q_4] \quad (C.16)$$

The virtual work done by the string forces, Eqs. (C.5) to (C.10), during the virtual displacement, Eqs. (C.11) to (C.16) is given by

$$\begin{aligned} \delta W = & -k\alpha_m(s)\alpha_n(s)[(q_1 + 0 \cdot q_2)(\delta q_3 + 0 \cdot \delta q_4) \\ & + (\cos n\pi/3 \cdot q_1 + \sin n\pi/3 \cdot q_2)(\cos n\pi/3 \cdot \delta q_3 + \sin n\pi/3 \cdot \delta q_4) \\ & + (\cos 2n\pi/3 \cdot q_1 + \sin 2n\pi/3 \cdot q_2)(\cos 2n\pi/3 \cdot \delta q_3 + \sin 2n\pi/3 \cdot \delta q_4) \\ & + (\cos n\pi \cdot q_1 + \sin n\pi \cdot q_2)(\cos n\pi \cdot \delta q_3 + \sin n\pi \cdot \delta q_4) \\ & + (\cos 4n\pi/3 \cdot q_1 + \sin 4n\pi/3 \cdot q_2)(\cos 4n\pi/3 \cdot \delta q_3 + \sin 4n\pi/3 \cdot \delta q_4) \\ & + (\cos 5n\pi/3 \cdot q_1 + \sin 5n\pi/3 \cdot q_2)(\cos 5n\pi/3 \cdot \delta q_3 + \sin 5n\pi/3 \cdot \delta q_4) \end{aligned} \quad (C.17)$$

which can be put in the form

$$\delta W = -k\alpha_m(s)\alpha_n(s)[a_1q_1\delta q_3 + a_2q_1\delta q_4 + a_3q_2\delta q_3 + a_4q_2\delta q_4 \\ + \text{higher order terms}] \quad (\text{C.18})$$

Evaluation of the coefficients a_1 , a_2 , a_3 , and a_4 in Eq. (C.18) reveals that for certain combinations of m and n , they are not zero, indicating that coupling exists. The following modes, in addition to others involving higher m and n , are coupled: $m=2, n=4$; $m=2, n=8$; $m=4, n=8$; $m=5, n=7$; $m=5, n=11$; $m=7, n=11$; $m=8, n=10$. Since the functions in the coefficients repeat, there are infinite numbers of coupled modes.

SYMBOLS

D	Rigidity parameter defined by Eq. (2.16)
E	Young's modulus of elasticity
E_1, E_2, \dots, E_8	Error functions
F_u, F_v, F_w	External forces
h	Thickness
K	Stiffness
k	Thickness parameter defined by Eq..(2.64)
L	Length
M	Mass
m	Number of circumferential waves
\bar{M}	Generalized boundary force
$N_s, Q_s, M_\theta,$ $N_{\theta s}, \dots$	Stress resultants
\bar{N}	Generalized boundary force
r_L	Cone radius at major end
r_0	Cone radius at minor end
\bar{S}	Generalized boundary force
s	Longitudinal coordinate
\bar{T}	Generalized boundary force
t	Time
u, v, w	Components of displacement

U_n, V_n, W_n	Fourier coefficients
U	Strain energy
W	Work
α	Cone semi-vertex angle
α_i	Function of s in assumed u
β_i	Function of s in assumed v
Δ	Frequency parameter defined by Eq. (5.1)
γ_i	Function of s in assumed w
$\gamma_{s\theta}$	Shear strain
$\epsilon_\alpha, \epsilon_\beta, \epsilon_\gamma$	Error functions of s and e
$\epsilon_s, \epsilon_\theta$	Normal strain
θ	Circumferential coordinate
$\chi_s, \chi_\theta, \chi_{s\theta}$	Curvature
ν	Poisson's ratio
ρ	Density
ω	Frequency
Ω	Frequency parameter defined by Eq. (4.1)
$()'$	First partial derivative with respect to s
$()^\cdot$	First partial derivative with respect to θ
$(\dot{\ })$	First derivative with respect to time
$\delta()$	Variation of $()$
$()'' ()''' ()''''$	Higher partial derivatives with respect to s

REFERENCES

1. Bolotin, V. V., Nonconservative Problems of the Theory of Elastic Stability, Macmillan, New York, pp. 58-62, 1963.
2. Chao-tsien, Tang, "The Vibration Modes and Eigenfrequencies of Circular Conical (and Cylindrical) Shells," Scientia Sinica, V13, n8, pp. 1189-1209, 1964.
3. Flugge, Wilhelm, Stresses in Shells, Springer-Verlag, Berlin, 1960.
4. Hu, W. C. L., "A Survey of the Literature on the Vibrations of Thin Shells," NASA CR 58048, 1964.
5. Hu, W. C. L., "Comments on Vibrational Characteristics of Thin-Wall Conical Frustum Shells," AIAA Journal, V3, n6, p. 1213, 1965.
6. Hu, W. C. L., Gormley, J. F., and Lindholm, U. S., "Flexural Vibrations of Conical Shells with Free Edges," NASA CR 384, 1966.
7. Love, A. E. H., A Treatise on the Mathematical Theory of Elasticity, Fourth Edition, Dover, New York, 1944.
8. Matthews, J. B., "Natural Frequencies and Mode Shapes of Circular Cylindrical Shells Determined by a Modified Galerkin Procedure," Ph.D. Dissertation, University of Arizona, 1966.
9. Platus, D. H., "Conical Shell Vibrations," NASA TN D-2767, 1965.
10. Seide, Paul, "A Donnell-Type Theory for Asymmetrical Bending and Buckling of Thin Conical Shells," Journal of Applied Mechanics, V24, n4, pp. 547-552, 1957.
11. Singer, Josef, "On the Equivalence of the Galerkin and Rayleigh-Ritz Methods," Journal of the Royal Aeronautical Society, V66, p. 592, September 1962.

12. Watkins, J. D., and Clary, R. R., "Vibrational Characteristics of Some Thin-Walled Cylindrical and Conical Frustum Shells," NASA TN D-2729, 1965.

UNCLASSIFIED

Security Classification

DOCUMENT CONTROL DATA - R&D

(Security classification of title, body of abstract and indexing annotation must be entered when the overall report is classified)

1. ORIGINATING ACTIVITY (Corporate author) Space and Missile Systems Organization (SAMSO/SMTAX) Air Force Systems Command, U S Air Force Los Angeles, Calif 90045		2a. REPORT SECURITY CLASSIFICATION UNCLASSIFIED	
		2b. GROUP	
3. REPORT TITLE NATURAL FREQUENCIES AND MODE SHAPES OF THE TRUNCATED CONICAL SHELL WITH FREE EDGES			
4. DESCRIPTIVE NOTES (Type of report and inclusive dates) A study accomplished in partial fulfillment of requirements for the PhD degree, University of Arizona			
5. AUTHOR(S) (Last name, first name, initial) KRAUSE, Frederick A., Capt, USAF			
6. REPORT DATE January 1968		7a. TOTAL NO. OF PAGES 90	7b. NO. OF REFS 12
8a. CONTRACT OR GRANT NO. None		8a. ORIGINATOR'S REPORT NUMBER(S) SAMSO-TR-68-37	
b. PROJECT NO.		8b. OTHER REPORT NO(S) (Any other numbers that may be assigned this report)	
c.			
d.			
10. AVAILABILITY/LIMITATION NOTICES This document has been approved for public release and sale; its distribution is unlimited.			
11. SUPPLEMENTARY NOTES		12. SPONSORING MILITARY ACTIVITY Space and Missile Systems Organization Air Force Systems Command U S Air Force	
13. ABSTRACT Results from experimental studies concerning the natural frequencies and mode shapes of the thin truncated conical shell with free edges have not been consistent. Mode shapes from one study were found to have an equal number of nodes at the two free edges when vibrating in a given mode while in contrast a second study revealed an unequal number of nodes at the two cone edges. The theoretical results presented in this study are obtained through the use of a modified Galerkin procedure and are in agreement with the equal node experimental data. At the same time, the theoretical results have been used as a basis for explaining the opposing experimental data.			

DD FORM 1473
1 JAN 64

UNCLASSIFIED

Security Classification

14. KEY WORDS	LINK A		LINK B		LINK C	
	ROLE	WT	ROLE	WT	ROLE	WT
Vibrations						
Conical Shells						
Frequencies						
Mode Shapes						
Galerkin Method						

INSTRUCTIONS

1. **ORIGINATING ACTIVITY:** Enter the name and address of the contractor, subcontractor, grantee, Department of Defense activity or other organization (*corporate author*) issuing the report.
- 2a. **REPORT SECURITY CLASSIFICATION:** Enter the overall security classification of the report. Indicate whether "Restricted Data" is included. Marking is to be in accordance with appropriate security regulations.
- 2b. **GROUP:** Automatic downgrading is specified in DoD Directive 5200.10 and Armed Forces Industrial Manual. Enter the group number. Also, when applicable, show that optional markings have been used for Group 3 and Group 4 as authorized.
3. **REPORT TITLE:** Enter the complete report title in all capital letters. Titles in all cases should be unclassified. If a meaningful title cannot be selected without classification, show title classification in all capitals in parenthesis immediately following the title.
4. **DESCRIPTIVE NOTES:** If appropriate, enter the type of report, e.g., interim, progress, summary, annual, or final. Give the inclusive dates when a specific reporting period is covered.
5. **AUTHOR(S):** Enter the name(s) of author(s) as shown on or in the report. Enter last name, first name, middle initial. If military, show rank and branch of service. The name of the principal author is an absolute minimum requirement.
6. **REPORT DATE:** Enter the date of the report as day, month, year, or month, year. If more than one date appears on the report, use date of publication.
- 7a. **TOTAL NUMBER OF PAGES:** The total page count should follow normal pagination procedures, i.e., enter the number of pages containing information.
- 7b. **NUMBER OF REFERENCES:** Enter the total number of references cited in the report.
- 8a. **CONTRACT OR GRANT NUMBER:** If appropriate, enter the applicable number of the contract or grant under which the report was written.
- 8b, 8c, & 8d. **PROJECT NUMBER:** Enter the appropriate military department identification, such as project number, subproject number, system numbers, task number, etc.
- 9a. **ORIGINATOR'S REPORT NUMBER(S):** Enter the official report number by which the document will be identified and controlled by the originating activity. This number must be unique to this report.
- 9b. **OTHER REPORT NUMBER(S):** If the report has been assigned any other report numbers (*either by the originator or by the sponsor*), also enter this number(s).
10. **AVAILABILITY/LIMITATION NOTICES:** Enter any limitations on further dissemination of the report, other than those

imposed by security classification, using standard statements such as:

- (1) "Qualified requesters may obtain copies of this report from DDC."
- (2) "Foreign announcement and dissemination of this report by DDC is not authorized."
- (3) "U. S. Government agencies may obtain copies of this report directly from DDC. Other qualified DDC users shall request through _____."
- (4) "U. S. military agencies may obtain copies of this report directly from DDC. Other qualified users shall request through _____."
- (5) "All distribution of this report is controlled. Qualified DDC users shall request through _____."

If the report has been furnished to the Office of Technical Services, Department of Commerce, for sale to the public, indicate this fact and enter the price, if known.

11. **SUPPLEMENTARY NOTES:** Use for additional explanatory notes.

12. **SPONSORING MILITARY ACTIVITY:** Enter the name of the departmental project office or laboratory sponsoring (*paying for*) the research and development. Include address.

13. **ABSTRACT:** Enter an abstract giving a brief and factual summary of the document indicative of the report, even though it may also appear elsewhere in the body of the technical report. If additional space is required, a continuation sheet shall be attached.

It is highly desirable that the abstract of classified reports be unclassified. Each paragraph of the abstract shall end with an indication of the military security classification of the information in the paragraph, represented as (TS), (S), (C), or (U).

There is no limitation on the length of the abstract. However, the suggested length is from 150 to 225 words.

14. **KEY WORDS:** Key words are technically meaningful terms or short phrases that characterize a report and may be used as index entries for cataloging the report. Key words must be selected so that no security classification is required. Identifiers, such as equipment model designation, trade name, military project code name, geographic location, may be used as key words but will be followed by an indication of technical context. The assignment of links, rules, and weights is optional.